Title: Emergence of enzalutamide resistance in prostate cancer is associated with BCL-2 and IKKB dependencies

Running Title: BCL-2 and IKKB dependencies in Enzalutamide-resistant CRPC

Yi Liang[1], Sujeeve Jeganathan[2], Stefano Marastoni[1], Adam Sharp[3,4], Ines Figueiredo[4], Richard Marcellus[5], Amanda Mawson[6], Zvi Shalev[1], Aleksandra Pesic[1], Joan Sweet[7], Haiyang Guo[1], David Uehling[5], Bora Gurel[4], Antje Neeb[4], Housheng Hansen He[1], Bruce Montgomery[8], Marianne Koritzinsky[1,9], Samantha Oakes[6,13], Johann S. de Bono[3,4], Martin Gleave[11], Amina Zoubeidi[11], Bradly G. Wouters[1,10], Anthony M. Joshua[1,6,12,13]

Affiliations

1. Princess Margaret Cancer Centre, University Health Network, Toronto, Canada
2. Quality Control Analytical Excellence, Sanofi Pasteur, Toronto, Canada
3. Royal Marsden Hospital, Surrey, United Kingdom
4. The Institute of Cancer Research, London, United Kingdom
5. Drug Discovery Program, Ontario Institute for Cancer Research, Toronto, Canada
6. Garvan Institute of Medical Research, Sydney, Australia
7. Department of Laboratory Medicine and Pathobiology, University Health Network, Toronto, Canada
8. Department of Medicine and Oncology, University of Washington, Seattle Cancer Care Alliance, Seattle, WA, USA
9. Department of Radiation Oncology, Department of Medical Biophysics, Institute of Medical Science, University of Toronto, Toronto, Canada
10. Department of Radiation Oncology, Department of Medical Biophysics, University of Toronto, Ontario Institute for Cancer Research, Toronto, Canada
11. Department of Urologic Sciences and Vancouver Prostate Centre, University of British Columbia, Vancouver, Canada
12. Department of Medical Oncology, Kinghorn Cancer Centre, St Vincent's Hospital, Sydney, Australia
13. Faculty of Medicine, UNSW Sydney, Australia

Corresponding author: Anthony M. Joshua
Address: Kinghorn Cancer Centre, 370 Victoria St, Darlinghurst, 2010, Sydney, Australia
Email: anthony.joshua@svha.org.au

Conflicts of interest

AMJ has received research funding (Institution) from Merck Serono, MSD, AstraZeneca, Roche, Eli-Lilly, Corvus, Janssen Oncology, Mayne Pharma, Marcogenics and Pfizer. AMJ has acted in a consultant or advisory role (Institution- no personal income) to Iqvia, BMS, Novartis, Ipsen, Noxopharm, Neolukin, AstraZeneca, Janssen Oncology, Sanofi, Pfizer

AS, IF, AN, BG and JdB are employees of the ICR, which has a commercial interest in abiraterone. AS has received travel support from Sanofi and Roche-Genentech, and speakers honorarium from Astellas Pharma. JdB has served on advisory boards and received fees from many companies including Astra Zeneca, Astellas, Bayer, Boehringer Ingelheim, Cellcentric, Daiichi, Genentech/Roche, Genmab, GSK, Janssen, Merck Serono, Merck Sharp & Dohme, Menarini/Silicon Biosystems, Orion, Pfizer, Qiagen, Sanofi Aventis, Sierra Oncology, Taiho, Vertex Pharmaceuticals. He is an employee of the ICR, which have received funding or other support for his research work from AZ, Astellas, Bayer, Cellcentric, Daiichi, Genentech, Genmab, GSK, Janssen, Merck Serono, MSD, Menarini/Silicon Biosystems, Orion, Sanofi Aventis, Sierra Oncology, Taiho, Pfizer, Vertex, and which has a commercial interest in abiraterone, PARP inhibition in DNA repair defective cancers and PI3K/AKT pathway inhibitors (no personal income). He was named as an inventor, with no financial interest, for patent 8,822,438. He has been the CI/PI of many industry sponsored clinical trials. JDB is a NIHR Senior Investigator. The views expressed are those of the authors and not necessarily those of the NIHR or Department of Health and Social Care.

Translational Relevance

Prostate cancer is the second most common carcinoma in North American men and one of the leading causes of cancer-related death. Patients with advanced and metastatic prostate cancer are typically treated with medical/surgical castration, as well as anti-androgen therapies including abiraterone acetate and enzalutamide either in the hormone sensitive or resistant settings. Developing novel therapeutic options that augment the activity of these agents is an urgent clinical need. In the present study, we identified that BCL-2 and IKKB inhibitors could specifically treat ENZ-resistance through a high-throughput pharmacological screen. In addition, BCL-2 or IKKB blockade prevented the emergence of ENZ resistance in xenograft models. Validation in clinical samples from men with mCRPC suggested greater relevance of the IKKB pathway. Our findings implicate the development of BCL-2 and IKKB dependencies in ENZ-resistant prostate cancer cell lines, and highlight the need for human tissue validation studies in the development of prostate cancer therapeutics.

Abstract

Purpose: Although enzalutamide (ENZ) has been widely used to treat *de novo* or castration-resistant metastatic prostate cancer, resistance develops, and disease progression is ultimately inevitable. There are currently no approved targeted drugs to specifically delay or overcome ENZ-resistance.

Experimental Design: We selected several ENZ-resistant cell lines that replicated clinical characteristics of the majority of patients with ENZ-resistant disease. A high-throughput pharmacological screen was utilized to identify compounds with greater cytotoxic effect for ENZ-resistant cell lines, compared to parental ENZ-sensitive cells. We validated the potential hits *in vitro* and *in vivo*, and used knock-down and over-expression assays to study the dependencies in ENZ-resistant prostate cancer.

Results: ABT199 (BCL-2 inhibitor) and IMD0354 (IKKB inhibitor), were identified as potent and selective inhibitors of cell viability in ENZ-resistant cell lines *in vitro* and *in vivo* which were further validated using loss-of-function assays of BCL-2 and IKKB. Notably, we observed that overexpression of BCL-2 and IKKB in ENZ-sensitive cell lines was sufficient for the emergence of ENZ resistance. In addition, we confirmed that BCL-2 or IKKB inhibitors suppressed the development of ENZ resistance in xenografts. However, validation of both BCL-2 and IKKB in matched castration-sensitive/resistant clinical samples showed that, concurrent with the development of enzalutamide/abiraterone resistance in patients, only the protein levels of IKKB were increased.

Conclusions: Our findings identify BCL-2 and IKKB dependencies in clinically relevant ENZ-resistant prostate cancer cells *in vitro* and *in vivo* but indicate that IKKB upregulation appears to have greater relevance to the progression of human castrate resistant prostate cancer.

Introduction

Other than skin cancer, prostate cancer is the most common cancer in North American males and the second leading cause of cancer-related deaths (1). Androgen Deprivation therapy, as well as anti-androgen therapies (such as enzalutamide (ENZ) and abiraterone acetate (AA)), are now well-established treatments for both *de novo* and castration-resistant metastatic disease (2,3). Unfortunately, despite significant efficacy, these therapies are not curative, and resistance inevitably develops (4,5). For example, in the castrate resistant setting with enzalutamide, the median time to PSA progression is only approximately 11 months (6,7). Previous studies have suggested several possible mechanisms of ENZ-resistance including androgen receptor gene amplifications, mutations, and/or splice variants, activation of other pro-survival or proliferation pathways including PI3K/AKT (8), MEK/ERK (9) and glucocorticoid receptor (10), or transformation into a neuroendocrine phenotype (11). There remains a need for additional therapeutic strategies to delay the emergence of resistance, and to identify putative biomarkers and targets that may indicate a higher probability of de novo or acquired resistance. In this study, we carried out a chemical screen and identified two drugs, Venetoclax (ABT199) and IMD0354, targeting BCL-2 and IKKB respectively, as potential therapies to target ENZ-resistant prostate cancer *in vitro* and *in vivo*. We subsequently validated both the drugs and their genomic targets in several pre-clinical assays and prostate cancer samples, to provide a basis for future clinical development.

Material and Methods

Cell lines and inhibitors

Human ENZ-sensitive, castration-resistant prostate cancer cell line $16D^{CRPC}$ and ENZ-resistant, castration-resistant prostate cancer cell lines including $34B^{ENZR}$, $40C^{ENZR}$ and $30C^{ENZR}$ were acquired from the Vancouver Prostate Centre and derived as previously described (12). They were maintained in RPMI-1640 supplemented with 10% fetal bovine serum (FBS) at 37^0C in 5% CO_2 atmosphere. Regular cell-line authentication was done by short-tandem repeat profiling. Mycoplasma testing was routinely done with the MycoAlert Mycoplasma Detection Kit (LT07-118, Lonza). ENZ-resistant cells were routinely tested for their resistance by growing them in 20 μM ENZ for 2-week periods and quantifying their growth rates. All ENZ-resistant and ENZ-sensitive lines were also routinely tested for their ability to grow in phenol red-free RPMI-1640 supplemented with 10% charcoal-stripped serum and quantifying their growth rates. Unless otherwise

indicated, cells used for growth assays and drug screens, were plated in media supplemented with 10% charcoal-stripped serum. Where appropriate in assays, ENZ concentration was 20 μM. Enzalutamide, ABT199 and IMD0354 were purchased from Selleck Chemicals (Houston, TX). For experiments, cells were plated for 24 hours before media was replaced with fresh drugs. Cells were incubated for 5-6 days without further media changes.

Drug screening assay

Four prostate cancer cell lines ($16D^{CRPC}$, $34B^{ENZR}$, $40C^{ENZR}$ and $30C^{ENZR}$) were dissociated into single cells and seeded at 1000-1500 cells/well in 50 μl RPMI-1640 medium (supplemented with 10% charcoal stripped serum) in 384-well microplates. Compounds were dissolved in DMSO as 10 mM stocks. Compound addition was performed at Ontario Institute for Cancer Research (OICR) using HP Tecan D300 digital dispenser. For each compound, 12-point, 2-fold serial dilutions were performed. Drug effects were compared to cells optimally proliferating in 0.1% DMSO alone, while wells filled with media served as background. CellTiter-Glo® (5 Ml, Promega) was added after five days, and fluorescence intensity measured after 20 minutes on a PHERAstar microplate reader, equipped with a λ540 excitation / λ590 emission filter.

Proliferation and Annexin-V/PI assays

Cells were seeded into black, clear-bottom 96-well assay plates or 6-well plates (for Annexin-V/PI assays) and incubated for 24 hours prior to treatment with serially increasing concentrations of enzalutamide, ABT199 or IMD0354. After five days of exposure to drugs, Alamar Blue® (Life Technologies) reagent was added and incubated for 4 hours. Fluorescence intensity was measured, and inhibition of proliferation was calculated by normalizing to an untreated control. Apoptotic cells were analyzed by FACS using the BioVision Annexin-V/PI kit as per the manufacturer's instructions.

Soft agar assay

Wells in 96-well assay plates were coated by 0.6% agar. Cells (100/well) were seeded in 0.4% agar with DMSO, ABT199 or IMD0354 in RPMI-1640 supplemented with 10% FBS (complete media). 0.5% agar in complete media with DMSO or inhibitors were covered on top of the cells. After 14-day incubation at 37^0C in 5% CO2 atmosphere,

bright-field pictures were captured under microscope. Alamar Blue® (Life Technologies) reagent was added and incubated for 4 hours. Fluorescence intensity was measured, and fold changes were calculated by normalizing to the DMSO control of $16D^{CRPC}$ cells.

Knocking-down and overexpression

The plasmids of BCL-2-GFP and IKKB-mCherry were purchased from GeneCopoeia (Rockville, MD). Plasmid transfection was performed with Lipofectamine 3000 (Life Technologies) in accordance with the manufacturer's guidelines. The siRNAs targeting BCL-2 and IKKB were purchased from Dharmacon (Horizon Discovery). Transfection of siRNAs at multiple concentrations was performed with Lipofectamine RNAiMAX (Life Technologies) in accordance with the manufacturer's guidelines.

Western blot analysis

Cells were washed twice with cold PBS and scraped in 50 mM Tris HCl pH 8.0, 150 mM NaCl, 1% NP-40, 0.5% sodium deoxycholate and 0.1% SDS supplemented with protease and phosphatase inhibitors (Roche). Lysates were clarified by centrifugation and protein concentration determined via BCA. 20-60μg reduced protein was resolved by NuPAGE 12% gels (Life Technologies) in MES gel running buffer. Proteins were transferred onto PVDF membrane, blocked with 5% skim milk and probed overnight at $4^{O}C$ with antibodies listed in Supplementary Table 1. Bound protein was visualized using HRP-conjugated secondary antibodies (GE Healthcare) and chemiluminesence. Western blots analyzed using the mean greyscale value of inverted scanned Western blots in Adobe Photoshop, and analysis of variance performed with the use of PRISM7 for MacOSX.

RNA extraction and quantitative RT-PCR

RNA was isolated using TRI reagent (Sigma) and samples were reverse transcribed using qScript cDNA SuperMix (Quantas). Quantitative real-time PCR was performed on an Eppendorf Realplex mastercycler using SYBR green (Quantas). Specific primers used are listed in Supplementary Table 2.

Murine prostate tumor xenograft model

Male NOD/SCID mice (4-6 weeks old) were anaesthetized using 2% isoflurane (inhalation) and 1 X 10^6 $16D^{CRPC}$ or $30C^{ENZR}$ prostate cancer cells suspended in 100 μl of PBS with 50% Matrigel (BD Biosciences) were implanted subcutaneously into the dorsal

flank on the right side of the mice. Once the tumors reached a palpable stage (~200 mm^3), the animals were randomized and treated with vehicle (DMSO), 10 mg/kg enzalutamide (dissolved in DMSO), 100 mg/kg ABT199 (dissolved in 50% PEG300 + 5% Tween 80 + ddH_2O) or 10 mg/kg IMD0354 (dissolved in 5% Tween 80 + 0.5% carboxymethyl cellulose + ddH_2O) intraperitoneally, every other day. Growth in tumor volume was recorded using digital calipers, and tumor volumes were estimated using the formula ($\pi/6$) (L X W^2), where L is the length of tumor and W is the width. Animal survival was determined based on the tumor sizes reaching maximal volumes allowable (1,500 mm^3) under the University Health Network Institutional Animal Care and Use Committee (IACUC). At the endpoint, mice were sacrificed, and tumors were extracted. All cells planned for inoculation into mice require the authentication of being free of all mycoplasma contamination. Typically, qPCR profiling of mycoplasma contamination was performed prior to inoculation. All experimental procedures were approved by the University Health Network IACUC under the protocol AUP 5643.

Patients and tissue samples

Patients were identified from a population of men with castration-resistant prostate cancer (CRPC) treated at the Royal Marsden NHS Foundation Trust (RMH) in accordance with the Declaration of Helsinki. All patients had given written informed consent and were enrolled in institutional protocols approved by the RMH (London, UK) ethics review committee. Twenty (20) patients with sufficient formalin-fixed, paraffin embedded (FFPE) diagnostic (archival) castration-sensitive prostate cancer (CSPC) biopsies, and matched FFPE CRPC biopsies were identified. All CSPC biopsies demonstrated adenocarcinoma and were from prostate needle biopsies (15), transurethral resection on the prostate (TURP; 1), prostatectomy (2), transurethral resection on the bladder (1) and a neck mass (1). CRPC tissue was obtained from metastatic biopsies of bone (9), lymph node (8), TURP (1) and pelvis (soft tissue; 2). All tissue blocks were freshly sectioned and only considered for IHC analyses if adequate material was present (≥50 tumour cells; reviewed by B.G.). Demographic and clinical data for each patient were retrospectively collected independently from the hospital electronic patient record system.

Tissue analysis

Immunohistochemistry (IHC) for BCL-2 and IKKB was performed on patient samples described above. BCL-2 IHC was performed using the mouse anti-BCL-2 monoclonal

antibody (Dako; M0887). Briefly, antigen retrieval was performed for 10 minutes with Bond ER2 solution (Leica Biosystems) and anti-BCL-2 antibody (1:750 dilution) incubated with tissue for 15 minutes and the reaction visualized using Bond Polymer Refine (Leica Biosystems) system. Appendix tissue was used as a positive control. Cell pellets from LNCaP95 cells treated with control and BCL-2 siRNA were used to confirm specificity of the antibody for BCL-2 (Supplementary Fig. S1). Mouse IgGs were used as negative controls. IKKB IHC was performed using the rabbit anti-IKKB monoclonal antibody (Cell Signaling Technologies; D30C6). Briefly, antigen retrieval was performed for 10 minutes with Bond ER2 solution (Leica Biosystems) and anti-IKKB antibody (1:500 dilution) incubated with tissue for 15 minutes and the reaction visualized using Bond Polymer Refine (Leica Biosystems) system. Appendix tissue was used as a positive control. Cell pellets from DU145 cells treated with control and IKKB siRNA were used to confirm specificity of the antibody for IKKB (Supplementary Fig. S2). Rabbit IgGs were used as negative controls.

Cytoplasmic BCL-2 and IKKB protein expression was determined for each case by a pathologist blinded to clinical data using the modified H score (HS) method; a semi-quantitative assessment of staining intensity that reflects antigen concentration. HS was determined according to the formula: [(% of weak staining) × 1] + [(% of moderate staining) × 2] + [(% of strong staining) × 3], yielding a range from 0 to 300.

Statistical analysis

HS were reported as median values with interquartile range (IQR). For paired, same patient, CSPC and CRPC expression studies the Wilcoxon matched-pair signed rank test (nonparametric; BCL-2) or paired student t-test (parametric; IKKB) was used to compare differences in cytoplasmic protein expression levels. All analyses were conducted, and graphs were generated, using GraphPad Prism v6.

Results

ENZ-resistant cell lines show greater tolerance to ENZ and exhibit T878A & F877L AR point mutation

ENZ-sensitive CRPC cell line $16D^{CRPC}$ and ENZ-resistant cell lines $34B^{ENZR}$, $40C^{ENZR}$, and $30C^{ENZR}$ were established from LNCaP xenografts as previously described (12) (Supplementary Fig. S3A). Initially, we characterized the three ENZ-resistant cell lines

34B^{ENZR}, 40C^{ENZR}, and 30C^{ENZR}, along with the ENZ-sensitive line 16D^{CRPC}. While all four lines had similar growth kinetics (Supplementary Fig. S3B), the ENZ-resistant lines consistently showed greater tolerance to higher ENZ concentrations (mean IC_{50} ranged from 49.7 to 50.8 μM) when compared to the ENZ-sensitive 16D^{CRPC} line (mean IC_{50} of 12.3 μM) or the hormone-sensitive LNCaP parental line (mean IC_{50} 9.6 μM, Supplementary Fig. S3C and D). All tested cell lines were AR and PSA positive (Supplementary Fig. S3E), and neither the ENZ-resistant 40C^{ENZR}/30C^{ENZR} lines nor the ENZ-sensitive 16D^{CRPC} line expressed AR-V7 (Supplementary Fig. S3F and G) or neuroendocrine biomarkers including synaptophysin (SYP) and neuron-specific enolase (NSE) (Supplementary Fig. S3H). However, we identified the known AR point mutation T878A (formerly T877A) in both LNCaP and all the derivative cell lines. Furthermore, all the ENZ-resistant cell lines (34B^{ENZR}, 40C^{ENZR}, and 30C^{ENZR}) harboured a heterozygous mutation F877L (formerly F876L, Supplementary Fig. S3I), which has been reported to be a possible inducer of ENZ-resistance (14,15).

Drug screening: ENZ-resistant lines show greater sensitivity to BCL-2 and IKKB inhibition.

To identify small-molecule inhibitors that may be used to target ENZ resistance, we carried out pharmacological screens using the CellTiter-Glo® assay on the ENZ-sensitive line and the three ENZ-resistant lines. Our compound pool consisted of two libraries, 'OICR Kinase Inhibitor Library' (480 compounds) and 'OICR Tool Compound Library' (300 compounds) (Supplementary Table 3). The initial screen with the two libraries was performed using 40C^{ENZR} and 30C^{ENZR} cell lines, in a randomized-plating manner (Supplementary Fig. S4A). The drug effects were classified into four subsets: 'cytotoxic', 'inactive', 'partial response' and 'cytostatic' (Supplementary Fig. S4B). For all the 184 compounds that were classified as 'cytotoxic' in both 40C^{ENZR} and 30C^{ENZR} (Supplementary Fig. S4C), we performed a secondary screen using all the four cell lines including 16D^{CRPC}, 34B^{ENZR}, 40C^{ENZR} and 30C^{ENZR}. To identify inhibitors that specifically target ENZ-resistant cells, we compared the IC50 values for 16D^{CRPC} and the mean IC50 values of the three ENZ-resistant cell lines (IC50 $Mean_{ENZR}$), and excluded those compounds that had lower IC50 values to 16D^{CRPC} cell line compared to any of the ENZ-resistant cell lines (138 compounds left, Supplementary Fig. S4D). To meet the criteria that the inhibitors should have at least 2-fold greater effect to the ENZ-resistant lines compared to the ENZ-sensitive line, i.e. IC50 $Mean_{ENZR}$ / IC50 (16D^{CRPC}) < 0.5, the secondary pharmacological screen identified only two hits: Venetoclax (ABT199), a BCL-2 inhibitor, and IMD0354, an IKKB inhibitor (Supplementary Fig. S4E). BCL-2 is

an anti-apoptosis canonical member of the BCL-2 family of regulator proteins whilst IKKB (IKK-β, inhibitor of nuclear factor kappa-B kinase subunit beta) is an enzyme that serves as a protein subunit of IκB kinase.

Validation of BCL-2 or IKKB inhibitor effects

We used the Alamar Blue®-based proliferation assays to validate the *in vitro* effect of ABT199 and IMD0354. For ABT199, the mean IC_{50} ranged from 0.67 to 0.76 μM for the ENZ-resistant lines, much lower than the ENZ-sensitive line $16D^{CRPC}$ (mean IC_{50} of 35.3 μM) (Fig. 1A). For IMD0354, the mean IC_{50} ranged from 0.24 to 0.25 μM for the ENZ-resistant lines, compared to the mean IC_{50} of 0.64 μM for the ENZ-sensitive line $16D^{CRPC}$ (Fig. 1B). The two inhibitors have similar effects on ENZ-resistant cell lines in the presence or absence of ENZ (Fig. 1C and D). In contrast, both hormone sensitive (LNCaP) and castrate resistant ($16D^{CRPC}$) cells were not as sensitive as the ENZ-resistant lines to ABT199 or IMD0354 (Fig. 1E and F). We validated this finding using the Incucyte® Live-Cell Analysis Systems to measure the cell confluency. We observed that with the treatment of ABT199 or IMD0354, the cell growth of ENZ-resistant lines including $40C^{ENZR}$ and $30C^{ENZR}$ was significantly slowed down compared to ENZ-sensitive line $16D^{CRPC}$ (Supplementary Fig. S5A and B). These data suggest that ABT199 and IMD0354 decrease the cell proliferation of ENZ-resistant cell lines *in vitro*.

To determine if the sensitivity of the ENZ-resistant lines to ABT199 or IMD0354 is due to increased cell death, we performed trypan blue counts after exposure to either drug for 5 days. We found that there was a significantly higher percentage of trypan blue positive cells in the inhibitor-treated ENZ-resistant cell lines $40C^{ENZR}$ and $30C^{ENZR}$ when compared to the ENZ-sensitive line $16D^{CRPC}$ (Supplementary Fig. S5C). Also, the treatment of ABT199 or IMD0354 significantly repressed the soft agar-colony formation of $40C^{ENZR}$ and $30C^{ENZR}$ cells, compared to $16D^{CRPC}$ (Supplementary Fig. S5D and E). To assess the contribution of apoptosis to the cell death effect with ABT199 or IMD0354, we measured the protein cleavage of PARP1. Intriguingly, we observed that ABT199 triggered apoptosis in both $40C^{ENZR}$ and $30C^{ENZR}$ cells while IMD0354 did not (Supplementary Fig. S5F) despite evidence of cell death with trypan blue assays (Supplementary Fig. S5C). We used Annexin-V staining to further validate whether the cells will undergo apoptosis with the treatment of ABT199 at increasing concentrations (2.5~10 μM). All ENZ-resistant cell lines underwent apoptosis in response to increasing concentrations of ABT199, and the $30C^{ENZR}$ cells showed a significant increase in

sensitivity to the ABT199 at a concentration of 10 μM ($p < 0.0001$) (Supplementary Fig. S5G).

We interrogated the effect of ABT199 and IMD0354 on $16D^{CRPC}$ or $30C^{ENZR}$ subcutaneous xenografts *in vivo*. Consistent with the *in vitro* results, the growth of $16D^{CRPC}$-derived xenografts responded to the treatment of ENZ, but neither ABT199 nor IMD0354 alone (Fig. 1G), suggesting that the $16D^{CRPC}$ cells were not sensitive to the inhibitors *in vivo*. Surprisingly, the treatment of ABT199 or IMD0354 alone appeared to stimulate the growth of $16D^{CRPC}$ xenografts (Fig. 1G). For $30C^{ENZR}$-derived xenografts, in the presence of pharmacological castration with ENZ, we found that the tumors were resistant to ENZ as expected (Fig. 1H, ENZ + vehicle control). In contrast, the growth of $30C^{ENZR}$-derived xenografts was significantly diminished by the two inhibitors (ENZ + vehicle vs. ENZ + ABT199, $p < 0.001$; ENZ + vehicle vs. ENZ + IMD0354, $p < 0.001$), strongly implying the sensitivity of $30C^{ENZR}$ cells to ABT199 and IMD0354. The body weight of all the animals at the endpoint was equivalent, indicating that neither ABT199 nor IMD0354 adversely affected animals' well-being (Supplementary Fig. S5H). Taken together, the inhibition of BCL-2 and IKKB, by ABT199 and IMD0354 respectively, showed selective targeting of ENZ-resistant cell lines and decreased cell growth both *in vitro* and *in vivo*.

Knock-down of BCL-2 and IKKB mimics the effects seen via pharmacological inhibition.

To further validate the BCL-2 or IKKB inhibitor effects, we performed genetic manipulation for both BCL-2 and IKKB. We measured cell growth on ENZ-sensitive ($16D^{CRPC}$) and ENZ-resistant lines ($40C^{ENZR}$) when transfected with increasing concentrations of two independent siRNAs targeting BCL-2 or IKKB. The negative control siRNA did not affect the cell growth of either $16D^{CRPC}$ or $40C^{ENZR}$ (Fig. 2A). As we increased the concentration of siBCL-2 (Fig. 2B and C) or siIKKB (Fig. 2D and E), the ENZ-resistant cell line $40C^{ENZR}$ showed a greater repression of cell proliferation in a dose-dependent manner, compared to the ENZ-sensitive cell line $16D^{CRPC}$. We confirmed that the repression of cell growth with increased siRNA concentrations correlated with decreased levels of BCL-2 or IKKB proteins (Fig. 2F and G). These data suggest that the proliferation of ENZ-resistant cell lines is BCL-2 and IKKB dependent.

BCL-2 and IKKB are sufficient for the emergence of enzalutamide resistance.

To further explore the BCL-2 and IKKB dependencies in ENZ resistance, we initially determined the protein levels of BCL-2 and IKKB in the ENZ-sensitive cell line $16D^{CRPC}$ and two of the ENZ-resistant cell lines including $40C^{ENZR}$ and $30C^{ENZR}$, and observed that the protein level of BCL-2 and IKKB in $40C^{ENZR}$ and $30C^{ENZR}$ cells was much higher compared to $16D^{CRPC}$ (Fig. 3A). We generated $16D^{CRPC}$ variants overexpressing BCL-2, IKKB or both (Fig. 3B) which had similar growth kinetics as parental $16D^{CRPC}$ cells (Supplementary Fig. S6A), and showed greater tolerance to higher ENZ concentrations (mean IC_{50} ranges from 27.5 to 52.7 μM) compared to the parental $16D^{CRPC}$ line (mean IC_{50} of 10.5 μM) (Fig. 3C and D). When treated with 20 μM ENZ, the proliferation of $16D^{CRPC}$ was dramatically repressed (Fig. 3E), whereas the BCL-2 or IKKB-overexpressing lines were partially resistant to ENZ treatment (Fig. 3F and G). The dual-overexpressing variant showed complete ENZ resistance, comparable to the ENZ-resistant lines used previously (Fig. 3H and I and Supplementary Fig. S6B). The direct comparison for ENZ fold inhibition of cell viability between $16D^{CRPC}$ parental control and BCL-2 and/or IKKB-overexpressing cells is also significant (Supplementary Fig. S6C).

To further determine the role of IKKB in regulating ENZ resistance, we performed IKKB knock-down assays using the two previously used siIKKBs, and tested the cell growth in the presence of ENZ. When transfected with 20 nM siIKKBs, the ENZ-resistant $40C^{ENZR}$ cell line exhibited a greater sensitivity to ENZ (IC50: 17.58~19.01 μM vs. 58.27 μM of negative control), whereas the knock-down of IKKB did not change the ENZ sensitivity in ENZ-sensitive $16D^{CRPC}$ cell line (IC50: 10.91~12.81 μM vs. 11.93 μM of negative control, Supplementary Fig. S6D).

As IKKB presumably activates NF-κB pathway, we assessed the NF-κB activity by measuring the protein level of nuclear p65 and cytoplasmic IκBα. We observed no nuclear expression of p65 and no change of IκBα level between $16D^{CRPC}$ parental control and its variants overexpressing BCL-2 and/or IKKB (Supplementary Fig. S6E), indicating that the NF-κB pathway was not activated in this setting.

We also tested the expression of multiple AR downstream targets including KLK3, NKX3.1 and TMPRSS2 in the presence of ENZ in the $16D^{CRPC}$ cell variants, and found that the overexpression of BCL-2 and/or IKKB did not affect the decrease of all the three AR targets with the treatment of ENZ (Supplementary Fig. S6F), suggesting that the ENZ resistance induced by BCL-2 and/or IKKB overexpression may not be relevant to

canonical AR signaling. These data of overexpression and knock-down assays, especially the dual overexpression of BCL-2 and IKKB, suggest that the emergence of ENZ resistance in prostate cancer is driven by BCL-2 and IKKB.

BCL-2 or IKKB inhibitor prevent the development of ENZ resistance *in vivo*

To explore the effect of the inhibitors to prevent the emergence of de novo resistance, we treated the $16D^{CRPC}$ tumor-bearing mice with ENZ in combination with vehicle control, BCL-2 or IKKB inhibitor in two cohorts. For the first cohort, the drugs including ENZ, ABT199 and IMD0354 were administered to the animals when the tumor size reached 200 mm^2, the time before ENZ-resistance developed. We found that the treatment of ABT199 or IMD0354 could significantly repress the tumor growth when the lesion started to relapse from Day 28 (ENZ + Vehicle vs. ENZ + ABT199, $p < 0.01$; ENZ + Vehicle vs. ENZ + IMD0354, $p < 0.001$), suggesting that the inhibitor of BCL-2 or IKKB suppresses the development of ENZ-resistance in $16D^{CRPC}$ tumor-bearing mice (Fig. 4A and Supplementary Fig. S7A). For the second cohort, we explored the effect of the drugs on acquired ENZ-resistance. We treated the $16D^{CRPC}$ tumor-bearing mice with vehicle control or ENZ alone when the tumor size reached 200 mm^2. After the ENZ-treated tumors reached 300 mm^2 (meaning the emerged ENZ-resistance), we randomly grouped the animals and administered them the BCL-2 or IKKB inhibitor or vehicle control in addition. Consistently, we found the growth of the relapsed tumors was significantly slowed by the treatment with ABT199 or IMD0354 (ENZ + Vehicle vs. ENZ + ABT199, $p < 0.01$; ENZ + Vehicle vs. ENZ + IMD0354, $p < 0.05$) (Fig. 4B and Supplementary Fig. S7B). Setting 15 mm of tumor's length as endpoint, the Kaplan-Meier analysis showed that ENZ in combination with ABT199 or IMD0354 increased the endpoint-free survival of $16D^{CRPC}$ relapsed tumor-bearing mice, compared to the treatment of ENZ plus vehicle control ($p = 0.017$ and $p = 0.067$, respectively, Fig. 4C and D). Taken together, these results suggest that the BCL-2 or IKKB inhibitor not only prevents the emergence of ENZ resistance, but also targets the ENZ-resistant disease *in vivo*.

Subsequently, we tested the AR genotype for the xenograft samples collected at the endpoint, and found that in all cases no change from the implanted cells. All the relapsed $16D^{CRPC}$ tumors in which ENZ was treated alone harbored the same AR T878A mutation as the vehicle control-treated $16D^{CRPC}$ tumors (Supplementary Fig. S7C and D), whereas the ENZ-treated $30C^{ENZR}$ xenografts exhibited both T878A and F877L mutation, similar as the $30C^{ENZR}$ cells (Supplementary Fig. S7E). We examined the expression of AR-V7 in the $16D^{CRPC}$ xenograft tissues by qPCR, and found that AR-V7 expression also did not

change after the development of ENZ resistance in the ENZ-treated 16D^{CRPC} tumors (Supplementary Fig. S7F), which is consistent with the result in the ENZ-resistant cell lines including 30C^{ENZR} (Supplementary Fig. S3F and G). To determine whether the level of BCL-2 or IKKB correlates with the emergence of ENZ resistance, we measured the expression level of BCL-2 and IKKB by both qPCR and IHC assays among the xenograft tissues from the animals that develop ENZ resistance. For BCL-2, the mRNA levels in ENZ-resistant tissues were slightly upregulated, compared to the vehicle control tissues (Supplementary Fig. S7G), and the BCL-2 protein levels measured by IHC did not change (the HS values in all tested samples were defined as zero, data not shown). However, we observed an increased level of IKKB mRNA in 4 out of 5 animals with ENZ resistance (Supplementary Fig. S7G), and a strong uptrend for the IKKB protein level, determined by IHC for cytoplasmic IKKB expression, in the ENZ-resistant tumors (mean HS 250; 100.0-300.0), compared to the vehicle controls (mean HS 166.7; 0.0-200.0) (Supplementary Fig. S7H), consistent with the protein level of IKKB in cell lines (Fig. 3A). These *in vivo* data suggest that the inhibition of BCL-2 and IKKB disrupts the emergence of de novo ENZ resistance potentially driven by the upregulation of IKKB.

Profiling of BCL-2 family members

To further clarify the underlying mechanism of sensitivity to BCL-2 inhibitor in ENZ-resistant cell lines, we assessed the expression level of multiple BCL-2 family members in the ENZ-sensitive cell line 16D^{CRPC}, and the ENZ-resistant but ABT199-sensitive cell lines including 40C^{ENZR} and 30C^{ENZR}, as well as the parental cell line LNCaP. To determine which of the BCL-2 family proteins may be involved in the ABT-199-induced cell death, we measured the protein level of multiple BCL-2 family members, including BH3-only pro-apoptotic sensors, pro-survival proteins and apoptotic effectors, with and without the treatment of 10 μM ABT-199 (Fig. 5A). Intriguingly, the levels of BCL-2, BAK, and BAD were greater in untreated 40C^{ENZR} and 30C^{ENZR} cell lines compared to LNCaP and 16D^{CRPC} cells, with significantly higher levels of BCL-2 ($p < 0.01$), BAD ($p < 0.001$) and BIM ($p < 0.001$) observed in the 30C^{ENZR} cell line compared to all other lines, supporting their increased sensitivity to ABT-199 (Fig. 5B). These results suggest that BCL-2, BAD and BIM are potentially responsible for the sensitivity to ABT199 in the ENZ-resistant cell lines.

Changes in BCL-2 and IKKB level in paired samples of human metastatic CRPC

In order to examine the clinical utility of these findings, we explored whether the expression level of BCL-2 and IKKB was induced by AR targeting therapy in a cohort of twenty (20) prostate cancer patients who developed castration-resistant disease with paired archival (castration-sensitive) and metastatic castration-resistant tissue biopsies (Supplementary Table 4). H-Score (HS) were determined by IHC for cytoplasmic BCL-2 and IKKB protein expression in all patient biopsies (Fig. 6A and B). Cytoplasmic BCL-2 expression did not change significantly ($p = 0.11$) as patients progressed from CSPC (median; IQR: HS 0.0; 0.0-23.8) to CRPC (HS 0.0; 0.0-12.5) (Fig. 6C). In contrast, cytoplasmic IKKB expression increased significantly ($p = 0.003$) as patients progressed from CSPC (median; IQR: HS 60.0; 22.5-100.0) to CRPC (HS 110.0; 80.0-160.0), and in 15 out of 20 cases the IKKB level of CRPC was increased compared to the matched CSPC ones (Fig. 6D). We further classified the CRPC samples into 3 subgroups based on the treatment followed by biopsy collection: post-AA, post-ENZ and post-ENZ plus AA. For additional mechanisms known to cause ENZ resistance, we tested the nuclear expression of AR-V7, and observed that the expression pattern of BCL-2, IKKB and AR-V7 showed no difference between these 3 subgroups (Fig. 6E). Furthermore, we did a correlation analysis between nuclear AR-V7 and cytoplasmic IKKB expression, but not finding any correlation (Spearman's correlation coefficient $r = -0.06$, $p = 0.82$, Fig. 6F). These results suggest that, with the development of AA and/or ENZ resistance in patients, the cytoplasmic level of IKKB is enhanced, which is consistent with our *in vitro* data showing that the protein level of IKKB is much higher in ENZ-resistant cell lines (Fig. 3A).

Discussion

There is a pressing need to identify pathways that contribute to prostate cancer disease progression during and after effective androgen receptor blockade with drugs such as AA and ENZ. In this paper, we initially modelled resistance with LNCaP derivative cell lines that mimicked the majority of patients who relapse on AA and ENZ with an unchanged non-neuroendocrine phenotype that continues to produce PSA. Herein, we have shown that inhibition of either BCL-2 or IKKB is not only a strategy to selectively kill ENZ-resistant prostate cancer cell lines and xenografts, but also a potential approach to prevent the emergence of ENZ-resistance in xenografts. We found that although the increased sensitivity to IMD0354 in ENZ-resistant cell lines is more modest (IC50: 0.20~0.29 μM vs. 0.69 μM of $16D^{CRPC}$), compared to ABT199 (IC50: 0.49~0.82 μM vs. 34.86 μM of $16D^{CRPC}$), it still met the criteria to identify hits in the drug screen (IC50 ratio $Mean_{ENZR}/16D^{CRPC} < 0.5$, Supplementary Fig. S4E). Furthermore, we have identified that

while overexpression of either BCL-2 or IKKB can lead to partial ENZ resistance in cells that were previously sensitive, the overexpression of both can fully mimic ENZ resistance. Also, our results of BCL-2 profiling have suggested that several key members of BCL-2 family define the increased sensitivity to ABT-199 in ENZ-resistant cell lines.

Interestingly, our *in vivo* data suggested that the BCL-2 and IKKB inhibitors, especially IMD0354, appeared to induce the growth of $16D^{CRPC}$-derived xenografts when they were administered alone, compared to the vehicle control (Fig. 1G). This was not consistent with our *in vitro* results, such as Alamar Blue assays (Fig. 1A~D), colony-formation assays in soft agar (Supplementary Fig. S5D and E), and knock-down experiments (Fig. 2B~E), although is likely not relevant to clinical care as other *in vivo* experiments in this study showed that ABT199 or IMD0354 combined with ENZ could treat the acquired ENZ-resistance (Fig. 1H) and prevent the development of ENZ-resistance (Fig. 4), suggesting that the combination of ENZ and ABT199 or IMD0354 may have therapeutic potential.

Current publications have documented multiple AR-related mechanisms of ENZ resistance, one of which is the point mutation F877L (14,15). Our sequencing data identified the same mutation in all the ENZ-resistant cell lines including $34B^{ENZR}$, $40C^{ENZR}$, and $30C^{ENZR}$. However, in our xenograft experiment which were similar to the original serial passaging process that generated the $34B^{ENZR}$, $40C^{ENZR}$, and $30C^{ENZR}$ cell lines, we did not find that this mutation appeared in any xenograft samples obtained from the relapsed $16D^{CRPC}$ tumors after ENZ treatment (Supplementary Fig. S7D). These results show that F877L mutation is not universally present as a mechanism of ENZ resistance, confirming the heterogeneity of underlying mechanisms of ENZ resistance. Other studies from clinical materials have also indicated that F877L is not the only driving mutation of ENZ resistance (16,17).

IKKβ is one of two catalytic subunits that makes up the ***I***nhibitor of Nuclear ***K***appa B ***K***inase (IKK) complex. The complex includes another catalytic subunit, IKKα, and a regulatory subunit, NEMO (IKKγ). The major role of this kinase complex is to phosphorylate and inhibit the activities of the ***I***nhibitor of Nuclear ***K***appa ***B*** protein (IκB) family. The IκB family serves to inhibit the activity of ***N***uclear ***F***actor ***K***appa ***B*** (NF-κB) proteins by forming heterodimers and sequestering them in the cytoplasm. Therefore, IKKs serve as upstream activators of NF-κB signaling. The role of NF-κB in prostate cancer progression to a castration resistant state has been well documented (18-20). NF-κB functions as a master transcription factor that activates inflammatory

cytokines/chemokines and underpins the synthesis of genes implicated in cell survival and chemoresistance, angiogenesis and localized invasion (21-24). With ENZ-resistance in particular, NFκB2/p52 has been shown to regulate androgen receptor splice variants and upregulate glucose metabolism as means to mediate resistance (25). In our study however, NF-κB signaling was not important in the resistance phenotype (Supplementary Fig. S6E). The use of various inhibitors included in our compound library, such as Ro 106-9920, pyrrolidine dithiocarbamate and dimethylamino parthenolide, did not selectively target ENZ-resistance cell lines (data not shown). Therefore, the effect of IKKβ inhibition in our study may be through an NFκB-independent manner. While IκBs have been the traditional substrates for IKKβ, there is growing evidence that IKKβ targets a variety of substrates through NF-κB-independent mechanisms. Some of these substrates include β-catenin, IRS-1, Dok1, TSC1, Cyclin D1 and Aurora A (26). Given the evidence that knock-down of IKKB sensitize ENZ-resistant cell line $40C^{ENZR}$ to ENZ (Supplementary Fig. S6D), it may be possible that IKKB expression in prostate cancer can activate one or more of these alternate pathways leading to ENZ resistance. For example, the over-expression of Aurora A signaling has been reported to drive the emergence of ENZ-resistant neuroendocrine prostate tumors (27,28).

The expression and involvement of BCL-2 in prostate cancer and its association with the emergence of CRPC has been documented since the early 1990s (29-31). BCL-2 protein levels are often increased in tumor cells following androgen ablation therapy (32,33), and likely act to confer an apoptosis-resistant phenotype in the malignant population (34-36). Using RNA-seq analyses to test ENZ-resistant cells generated by a xenograft-based model, Li et al. also reported similarly that BCL-2 is highly up-regulated in ENZ-resistant prostate cancer, and that ABT199 can repress the tumor growth of ENZ-resistant xenografts (37). Relevant to this finding, one of the strengths of our study has been the ability to validate our findings in two clinical cohorts. In the larger cohort from the Royal Marsden, surprisingly, we detected no up-regulation in BCL-2 in the presence of AA/ENZ compared to the hormone sensitive samples using standard immunohistochemistry, which may imply that our pre-clinical findings have limited clinical relevance or limitations of our assay in small tissue samples. Current clinical trials exploring the utility of combining ENZ with Venetoclax (NCT 03751436) are quantifying this benefit. The IKKB expression levels in post-AA/ENZ treatment specimens exhibited a significant up-regulation compared to the pre-treatment CSPC counterparts (Fig. 6D), consistent with the *in vitro* data in the ENZ-resistant cell lines. The reason for the dissociation between the pre-clinical and clinical findings with BCL-2

reinforce the importance of validated pre-clinical findings in human tissue prior to embarking on clinical trials with targeted therapies.

Further research is required to understand the co-dependency of IKKB and BCL-2 in ENZ-resistance. Previous reports demonstrated that BCL-2 is transcriptionally regulated by the NF-κB pathway in prostate cancer (38), suggesting that BCL-2 is a downstream target gene of NF-κB signaling. However, we found that IKKB-overexpressing $16D^{CRPC}$ cell line had a similar sensitivity to ABT199, compared to the parental $16D^{CRPC}$ cells, and unlike ABT199 induced apoptosis, the type of cell death triggered by IMD-0354 remained uncharacterized (data not shown). Given that IKKB may be acting in a NF-κB-independent manner, we hypothesize that BCL-2 and IKKB may represent two independent mechanisms in the development of ENZ resistance.

Although multiple pathways likely converge to drive the emergence of ENZ resistance, understanding the contribution of BCL-2 and IKKB to this disease is critical for better implementation of current therapies for CRPC and may have implications across the disease spectrum in particular in *de novo* metastatic disease where outcomes remain inadequate despite recent therapeutic advances. Taken together, data from our drug screen and the accompanying *in vitro/vivo* validation implicate BCL-2 and IKKB dependencies in ENZ-resistant prostate cancer, suggesting their potential as novel therapeutic agents for the treatment of the disease, both of which require further validation and verification in larger human cohorts.

Acknowledgement

The work in this grant was supported by "Functional Assessment and Characterization of MDV3100-Resistant Cell Lines," Proposal Log Number PC110998, Award Number W81XWH-12-1-0239; Prostate Cancer Canada-Movember Team T2103-1; Rising Star in Prostate Cancer Research 2013 RS2013-58; Stanley Tessis Prostate Cancer Research Fund and Hold' em for Life Prostate Cancer Research Fund (AMJ)

The Oakes Laboratory is supported by Cancer Council NSW, Cue Clothing Co. and the Mostyn Family Foundation.

The de Bono laboratory is supported by research funding from Movember, Department of Defense, Prostate Cancer UK, Cancer Research UK, an Experimental Cancer Medicines Centres (ECMC) grant, Prostate Cancer Foundation and the National Institute for Health Research (NIHR) Biomedical Research Centre at the Royal Marsden NHS Foundation Trust (RMH) and the Institute of Cancer Research (ICR), London. AS has been supported by the Medical Research Council (MR/M018618/1), the Academy of Medical Sciences/Prostate Cancer UK (SGCL15) and a Prostate Cancer Foundation Young Investigator Award. The views expressed are those of the authors and not necessarily those of the NIHR or Department of Health and Social Care.

References

1. Jemal A, Siegel R, Ward E, Murray T, Xu J, Smigal C, et al. Cancer statistics, 2006. CA Cancer J Clin 2006;**56**:106-30.
2. Davis ID, Martin AJ, Stockler MR, Begbie S, Chi KN, Chowdhury S, et al. Enzalutamide with Standard First-Line Therapy in Metastatic Prostate Cancer. N Engl J Med 2019;**381**:121-31.
3. Hussain M, Tangen CM, Higano C, Schelhammer PF, Faulkner J, Crawford ED, et al. Absolute prostate-specific antigen value after androgen deprivation is a strong independent predictor of survival in new metastatic prostate cancer: data from Southwest Oncology Group Trial 9346 (INT-0162). J Clin Oncol 2006;**24**:3984-90.
4. Gleave M, Bruchovsky N, Goldenberg SL, Rennie P. Intermittent androgen suppression for prostate cancer: rationale and clinical experience. Eur Urol 1998;**34 Suppl 3**:37-41.
5. Gleave ME, Goldenberg SL, Chin JL, Warner J, Saad F, Klotz LH, et al. Randomized comparative study of 3 versus 8-month neoadjuvant hormonal therapy before radical prostatectomy: biochemical and pathological effects. J Urol 2001;**166**:500-6; discussion 6-7.
6. Beer TM, Armstrong AJ, Rathkopf D, Loriot Y, Sternberg CN, Higano CS, et al. Enzalutamide in Men with Chemotherapy-naive Metastatic Castration-resistant Prostate Cancer: Extended Analysis of the Phase 3 PREVAIL Study. Eur Urol 2017;**71**:151-4.
7. Chen CD, Welsbie DS, Tran C, Baek SH, Chen R, Vessella R, et al. Molecular determinants of resistance to antiandrogen therapy. Nat Med 2004;**10**:33-9.
8. Carver BS, Chapinski C, Wongvipat J, Hieronymus H, Chen Y, Chandarlapaty S, et al. Reciprocal feedback regulation of PI3K and androgen receptor signaling in PTEN-deficient prostate cancer. Cancer Cell 2011;**19**:575-86.
9. Toren P, Kim S, Johnson F, Zoubeidi A. Combined AKT and MEK Pathway Blockade in Pre-Clinical Models of Enzalutamide-Resistant Prostate Cancer. PLoS One 2016;**11**:e0152861.
10. Arora VK, Schenkein E, Murali R, Subudhi SK, Wongvipat J, Balbas MD, et al. Glucocorticoid receptor confers resistance to antiandrogens by bypassing androgen receptor blockade. Cell 2013;**155**:1309-22.
11. Parimi V, Goyal R, Poropatich K, Yang XJ. Neuroendocrine differentiation of prostate cancer: a review. Am J Clin Exp Urol 2014;**2**:273-85.

12. Bishop JL, Thaper D, Vahid S, Davies A, Ketola K, Kuruma H, et al. The Master Neural Transcription Factor BRN2 Is an Androgen Receptor-Suppressed Driver of Neuroendocrine Differentiation in Prostate Cancer. Cancer Discov 2017;**7**:54-71.
13. Montgomery B, Tretiakova MS, Joshua AM, Gleave ME, Fleshner N, Bubley GJ, et al. Neoadjuvant Enzalutamide Prior to Prostatectomy. Clin Cancer Res 2017;**23**:2169-76.
14. Korpal M, Korn JM, Gao X, Rakiec DP, Ruddy DA, Doshi S, et al. An F876L mutation in androgen receptor confers genetic and phenotypic resistance to MDV3100 (enzalutamide). Cancer Discov 2013;**3**:1030-43.
15. Joseph JD, Lu N, Qian J, Sensintaffar J, Shao G, Brigham D, et al. A clinically relevant androgen receptor mutation confers resistance to second-generation antiandrogens enzalutamide and ARN-509. Cancer Discov 2013;**3**:1020-9.
16. Azad AA, Volik SV, Wyatt AW, Haegert A, Le Bihan S, Bell RH, et al. Androgen Receptor Gene Aberrations in Circulating Cell-Free DNA: Biomarkers of Therapeutic Resistance in Castration-Resistant Prostate Cancer. Clin Cancer Res 2015;**21**:2315-24.
17. Lallous N, Volik SV, Awrey S, Leblanc E, Tse R, Murillo J, et al. Functional analysis of androgen receptor mutations that confer anti-androgen resistance identified in circulating cell-free DNA from prostate cancer patients. Genome Biol 2016;**17**:10.
18. Jin R, Yamashita H, Yu X, Wang J, Franco OE, Wang Y, et al. Inhibition of NF-kappa B signaling restores responsiveness of castrate-resistant prostate cancer cells to anti-androgen treatment by decreasing androgen receptor-variant expression. Oncogene 2015;**34**:3700-10.
19. Jin RJ, Lho Y, Connelly L, Wang Y, Yu X, Saint Jean L, et al. The nuclear factor-kappaB pathway controls the progression of prostate cancer to androgen-independent growth. Cancer Res 2008;**68**:6762-9.
20. Nunes JJ, Pandey SK, Yadav A, Goel S, Ateeq B. Targeting NF-kappa B Signaling by Artesunate Restores Sensitivity of Castrate-Resistant Prostate Cancer Cells to Antiandrogens. Neoplasia 2017;**19**:333-45.
21. Ammirante M, Luo JL, Grivennikov S, Nedospasov S, Karin M. B-cell-derived lymphotoxin promotes castration-resistant prostate cancer. Nature 2010;**464**:302-5.
22. Karin M. NF-kappaB as a critical link between inflammation and cancer. Cold Spring Harb Perspect Biol 2009;**1**:a000141.

23. Luo JL, Tan W, Ricono JM, Korchynskyi O, Zhang M, Gonias SL, et al. Nuclear cytokine-activated IKKalpha controls prostate cancer metastasis by repressing Maspin. Nature 2007;**446**:690-4.
24. Sharma J, Gray KP, Harshman LC, Evan C, Nakabayashi M, Fichorova R, et al. Elevated IL-8, TNF-alpha, and MCP-1 in men with metastatic prostate cancer starting androgen-deprivation therapy (ADT) are associated with shorter time to castration-resistance and overall survival. Prostate 2014;**74**:820-8.
25. Nadiminty N, Tummala R, Liu C, Yang J, Lou W, Evans CP, et al. NF-kappaB2/p52 induces resistance to enzalutamide in prostate cancer: role of androgen receptor and its variants. Mol Cancer Ther 2013;**12**:1629-37.
26. Chariot A. The NF-kappaB-independent functions of IKK subunits in immunity and cancer. Trends Cell Biol 2009;**19**:404-13.
27. Beltran H, Oromendia C, Danila DC, Montgomery B, Hoimes C, Szmulewitz RZ, et al. A Phase II Trial of the Aurora Kinase A Inhibitor Alisertib for Patients with Castration-resistant and Neuroendocrine Prostate Cancer: Efficacy and Biomarkers. Clin Cancer Res 2019;**25**:43-51.
28. Beltran H, Rickman DS, Park K, Chae SS, Sboner A, MacDonald TY, et al. Molecular characterization of neuroendocrine prostate cancer and identification of new drug targets. Cancer Discov 2011;**1**:487-95.
29. Liu AY, Corey E, Bladou F, Lange PH, Vessella RL. Prostatic cell lineage markers: emergence of BCL2+ cells of human prostate cancer xenograft LuCaP 23 following castration. Int J Cancer 1996;**65**:85-9.
30. Gleave M, Tolcher A, Miyake H, Nelson C, Brown B, Beraldi E, et al. Progression to androgen independence is delayed by adjuvant treatment with antisense Bcl-2 oligodeoxynucleotides after castration in the LNCaP prostate tumor model. Clin Cancer Res 1999;**5**:2891-8.
31. Miyake H, Tolcher A, Gleave ME. Antisense Bcl-2 oligodeoxynucleotides inhibit progression to androgen-independence after castration in the Shionogi tumor model. Cancer Res 1999;**59**:4030-4.
32. Fuzio P, Ditonno P, Lucarelli G, Battaglia M, Bettocchi C, Senia T, et al. Androgen deprivation therapy affects BCL-2 expression in human prostate cancer. Int J Oncol 2011;**39**:1233-42.
33. Lin Y, Fukuchi J, Hiipakka RA, Kokontis JM, Xiang J. Up-regulation of Bcl-2 is required for the progression of prostate cancer cells from an androgen-dependent to an androgen-independent growth stage. Cell Res 2007;**17**:531-6.

34. Yoshino T, Shiina H, Urakami S, Kikuno N, Yoneda T, Shigeno K, et al. Bcl-2 expression as a predictive marker of hormone-refractory prostate cancer treated with taxane-based chemotherapy. Clin Cancer Res 2006;**12**:6116-24.
35. Miayake H, Tolcher A, Gleave ME. Chemosensitization and delayed androgen-independent recurrence of prostate cancer with the use of antisense Bcl-2 oligodeoxynucleotides. J Natl Cancer Inst 2000;**92**:34-41.
36. Tolcher AW, Chi K, Kuhn J, Gleave M, Patnaik A, Takimoto C, et al. A phase II, pharmacokinetic, and biological correlative study of oblimersen sodium and docetaxel in patients with hormone-refractory prostate cancer. Clin Cancer Res 2005;**11**:3854-61.
37. Li Q, Deng Q, Chao HP, Liu X, Lu Y, Lin K, et al. Linking prostate cancer cell AR heterogeneity to distinct castration and enzalutamide responses. Nat Commun 2018;**9**:3600.
38. Catz SD, Johnson JL. Transcriptional regulation of bcl-2 by nuclear factor kappa B and its significance in prostate cancer. Oncogene 2001;**20**:7342-51.

Figure Legends

Figure 1. ENZ-resistant cell lines are more responsive to the pharmacological inhibition of BCL-2 and IKKB than ENZ-sensitive cells.

A~F. Cell viability after 6 days of growth in varying concentrations of ABT199 or IMD0354 without ENZ or with 20 μM ENZ, with IC50 values (μM) indicated at bottom. A. with ABT199 alone; B. with IMD0354 alone; C. with ABT199 and ENZ; D. with IMD0354 and ENZ. E. with ABT199 alone (the IC50 values could not be accurately determined within the scope of the experiment); F. with IMD0354 alone.

G. Tumor growth of $16D^{CRPC}$ xenografts with the treatment of vehicle control (DMSO), 10 mg/kg ENZ, 100 mg/kg ABT199 or 10 mg/kg IMD0354, when the tumor size exceeds 200 mm^3.

H. Tumor growth of $30C^{ENZR}$ xenografts with the treatment of vehicle control (DMSO), 100 mg/kg ABT199 or 10 mg/kg IMD0354, in combination with 10 mg/kg ENZ, when the tumor size exceeds 200 mm^3. ***, $p < 0.001$.

Figure 2. Knockdown of BCL-2 or IKKB mimics the effects of each inhibitor.

A~E. Growth kinetics of ENZ-sensitive $16D^{CRPC}$ cells (top) or ENZ-resistant $40C^{ENZR}$ cells (bottom) when transfected with increasing concentrations of negative control siRNA (siCtrl, A), siBCL-2 #1 (B), siBCL-2 #2 (C), siIKKB #1 (D) or siIKKB #2 (E).

F~G. Western blots confirming the knock-down efficiency for BCL-2 (F) and IKKB (G) in $16D^{CRPC}$ and $40C^{ENZR}$ cell lines. Untreated $40C^{ENZR}$ cells served as positive control of BCL-2 expression. β-Actin used as loading control.

Figure 3. BCL-2 and IKKB are sufficient for enzalutamide resistance.

A. Basal protein levels of BCL-2 and IKKB in cell lines. β-Actin used as loading control.

B. Western blots confirming the endogenous and artificial expression of BCL-2 and IKKB in $16D^{CRPC}$ cell line variants. Untreated $40C^{ENZR}$ cells served as positive control of endogenous BCL-2 expression. β-Actin used as loading control.

C. Representative curve of cell viability of $16D^{CRPC}$ cell line variants after 6 days of growth in varying concentrations of ENZ, with IC50 values (μM) indicated at bottom.

D. Means and standard deviations of ENZ IC50 of three independent experiments for each cell line. ***, $p < 0.001$.

E~H. Growth kinetics of $16D^{CRPC}$ cell line variants in the absence and presence of 20 μM ENZ. E. $16D^{CRPC}$ parental cells; F. $16D^{CRPC}$-BCL-2 variant; G. $16D^{CRPC}$-IKKB variant; H. $16D^{CRPC}$-2xOE variant expressing both BCL-2 and IKKB.

I. Quantification of cell confluency at last timepoint. *, $p < 0.05$.

Figure 4. BCL-2 or IKKB inhibitor prevents the development of ENZ-resistance *in vivo*.

A. Tumor growth of $16D^{CRPC}$-derived xenografts with the treatment of vehicle control (DMSO), 100 mg/kg ABT199 or 10 mg/kg IMD0354, in combination with 10 mg/kg ENZ, when the tumor size exceeds 200 mm^3. Means and standard errors of the mean (SEMs) are shown. **, $p < 0.01$. ***, $p < 0.001$. p-values were calculated using Bonferroni's multiple comparisons test.

B. Tumor growth of $16D^{CRPC}$-derived xenografts with the treatment of vehicle control (DMSO) or 10 mg/kg ENZ, when the tumor size exceeds 200 mm^3. After the size of ENZ-treated tumor reaches 300 mm^3, the mice are additionally treated with vehicle control (DMSO), 100 mg/kg ABT199 or 10 mg/kg IMD0354 (indicated). Means and standard errors of the mean (SEMs) are shown. *, $p < 0.05$. **, $p < 0.01$. p-values were calculated using Bonferroni's multiple comparisons test.

C. Survival curves reported as a Kaplan-Meier plot. Endpoint: 1,500 mm^3 of tumor's volume.

D. Statistical analyses for pair-wise comparison (log-rank test). p-values are indicated.

Figure 5. Protein level of BCL-2 family members.

A. Representative Western blots in LNCaP, $16D^{CRPC}$, $40C^{ENZR}$ and $30C^{ENZR}$ cell lines treated with vehicle or 10 μM ABT199 using antibodies to PUMAα, PUMAβ, NOXA, BIM, BAD, tBID, MCL-1, BCL-2, BCL-XL, BAX, BAK and α-tubulin as house-keeping control. kDa shown are that reporting in PhosphoSitePlus.

B. Bar graphs of densitometry from Panel A. 3-4 independent experiments, one-way ANOVA p-values are indicated.

Figure 6. BCL-2 and IKKB protein expression as prostate cancer patients develop treatment resistance.

A. Representative micrographs of BCL-2 detection by immunohistochemistry in matched diagnostic (archival) castration-sensitive prostate cancer (CSPC) and metastatic castration-resistant prostate cancer (CRPC) biopsies (scale bar: 100 μm).

B. Representative micrographs of IKKB detection by immunohistochemistry in matched diagnostic (archival) castration-sensitive prostate cancer (CSPC) and metastatic castration-resistant prostate cancer (CRPC) biopsies (scale bar: 100 μm).

C. Expression (H-score) of cytoplasmic BCL-2 expression in 20 patients with matched diagnostic (archival) CSPC (grey) and metastatic CRPC (red) biopsies. Left, median H-

score and interquartile range is shown. p-value was calculated using Wilcoxon matched-pair signed rank test. Right, demonstration with matched samples highlighted.

D. Expression (H-score) of cytoplasmic IKKB expression in 20 patients with matched diagnostic (archival) CSPC (grey) and metastatic CRPC (red) biopsies. Left, median H-score and interquartile range is shown. p-value was calculated using paired student t-test. Right, demonstration with matched samples highlighted.

E. Expression (H-score) of cytoplasmic IKKB, cytoplasmic BCL-2 and nuclear AR-V7 in 20 patients with metastatic CRPC biopsies was determined. Biopsies were divided by those biopsies taken following abiraterone acetate (AA, n = 9), enzalutamide (ENZ, n = 7) or both (A+E, n = 4). Median H-score, interquartile range and full range is shown. *, 2 biopsies missing. ^, 1 biopsy missing.

F. Expression (H-score) of cytoplasmic IKKB and nuclear AR-V7 in 17 patients with metastatic CRPC biopsies was determined. Biopsies taken following abiraterone acetate (grey), enzalutamide (blue) or both (orange) are shown. Spearman's correlation coefficient is shown.

Fig. 1

A

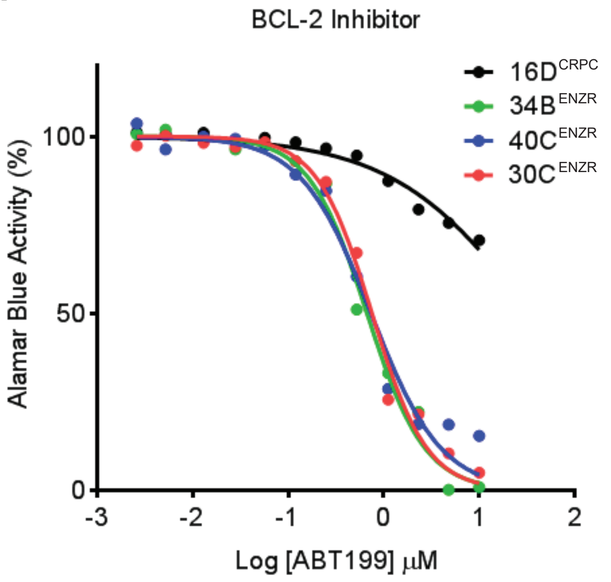

	16D CRPC	34B ENZR	40C ENZR	30C ENZR
IC50	35.26	0.6696	0.7398	0.7556

B

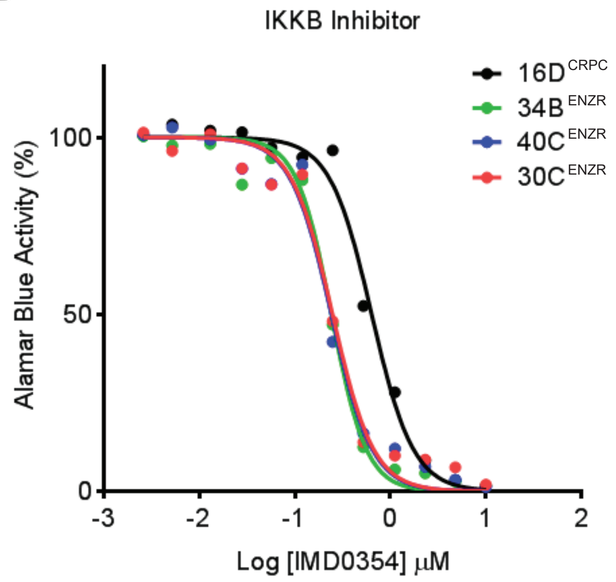

	16D CRPC	34B ENZR	40C ENZR	30C ENZR
IC50	0.6392	0.2423	0.2423	0.2488

C

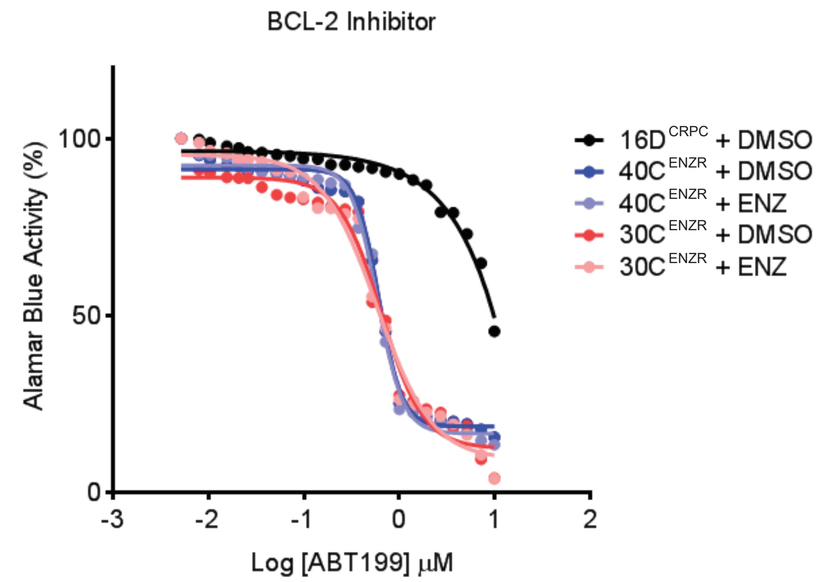

	16D CRPC + DMSO	40C ENZR + DMSO	40C ENZR + ENZ	30C ENZR + DMSO	30C ENZR + ENZ
IC50	~ 146648	0.6084	0.5913	0.6467	0.5878

D

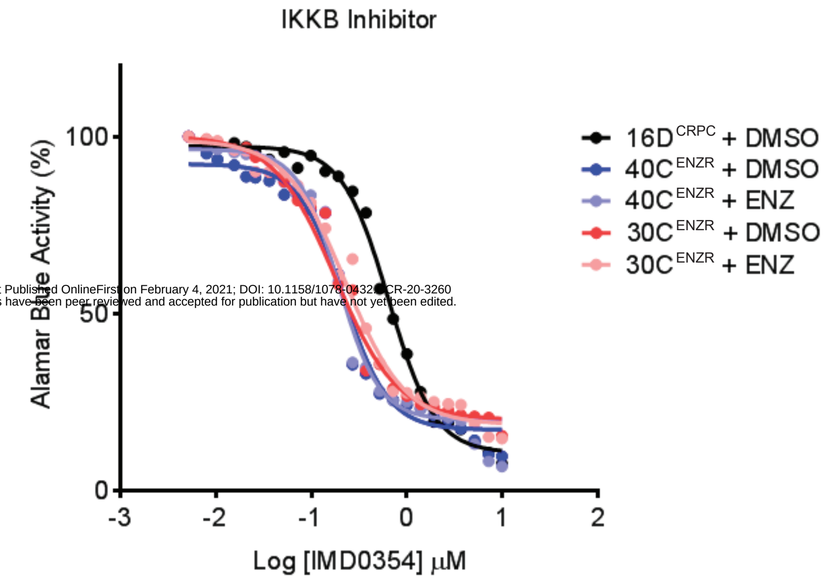

	16D CRPC + DMSO	40C ENZR + DMSO	40C ENZR + ENZ	30C ENZR + DMSO	30C ENZR + ENZ
IC50	0.6449	0.2170	0.1935	0.1790	0.2286

E

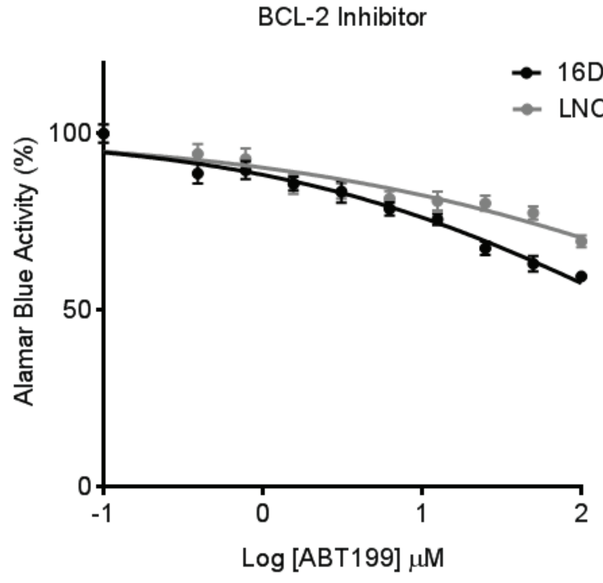

	LNCaP	16D CRPC
IC50	~ 1894	~ 231

F

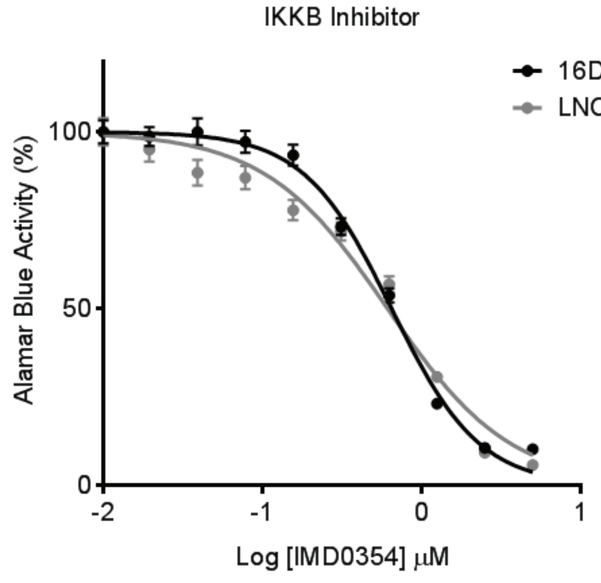

	LNCaP	16D CRPC
IC50	0.6133	0.6494

G

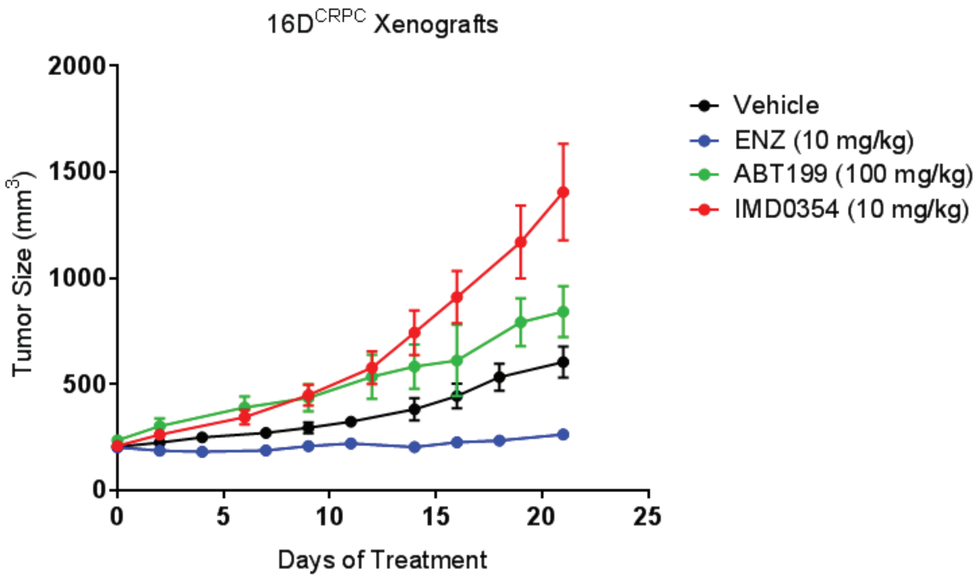

H

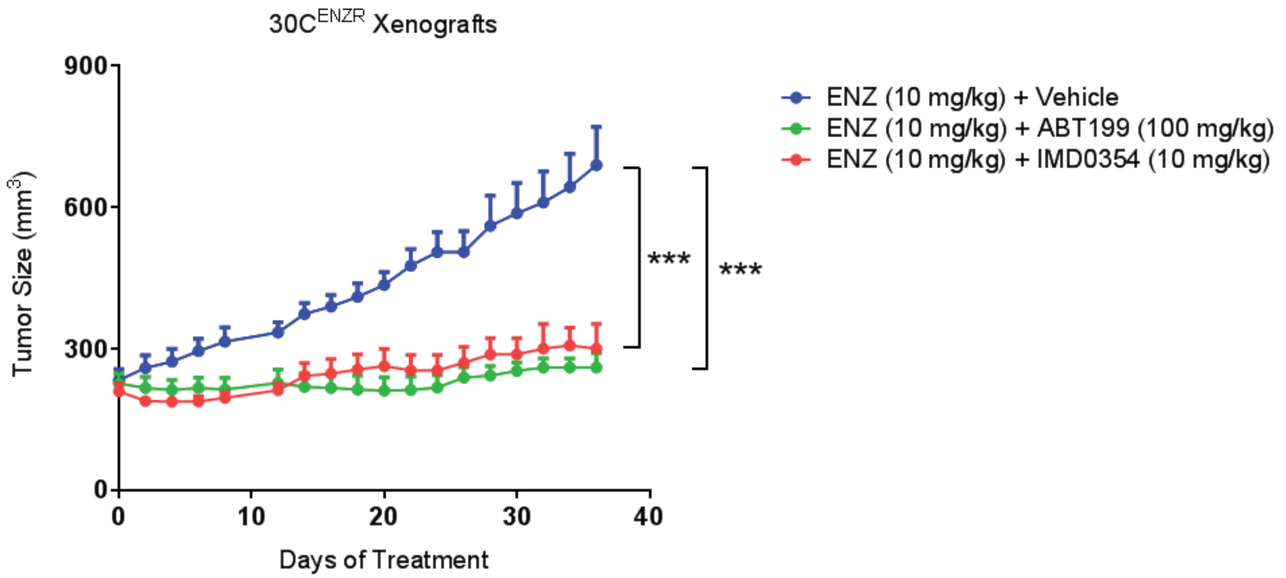

Fig. 2

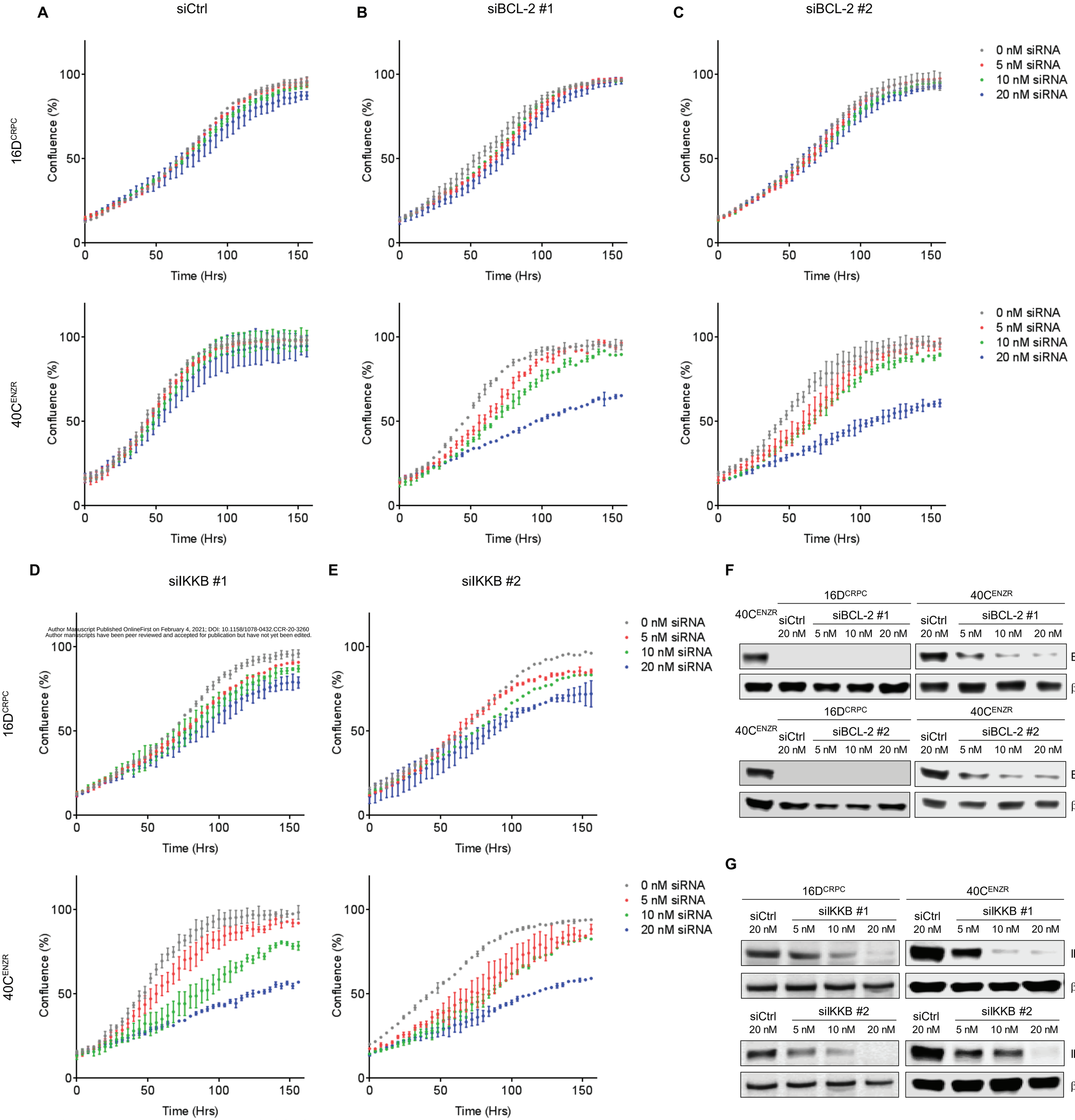

Fig. 3

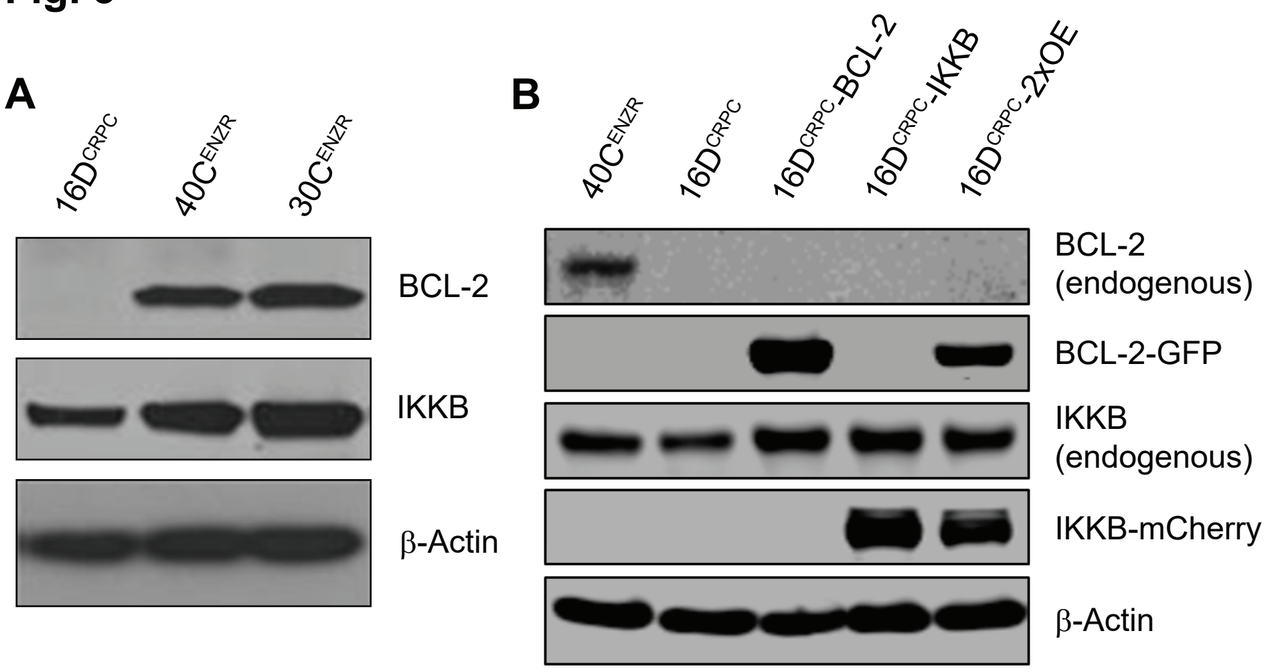

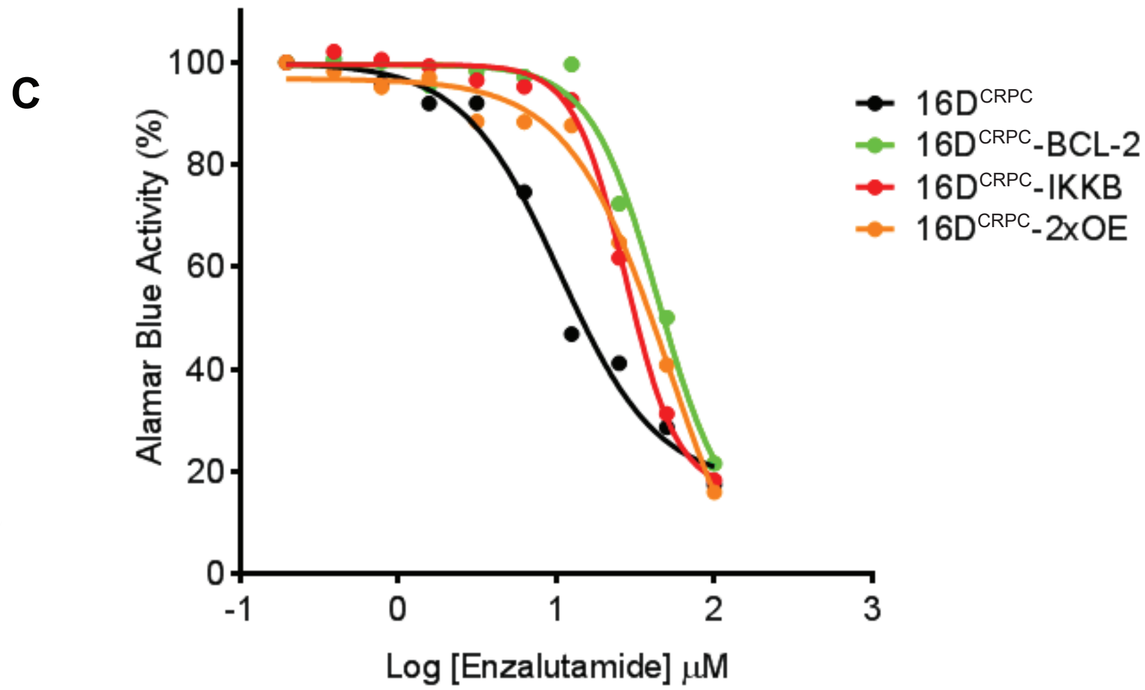

	16D^{CRPC}	16D^{CRPC}-BCL-2	16D^{CRPC}-IKKB	16D^{CRPC}-2xOE
IC50	10.52	43.99	27.48	52.73

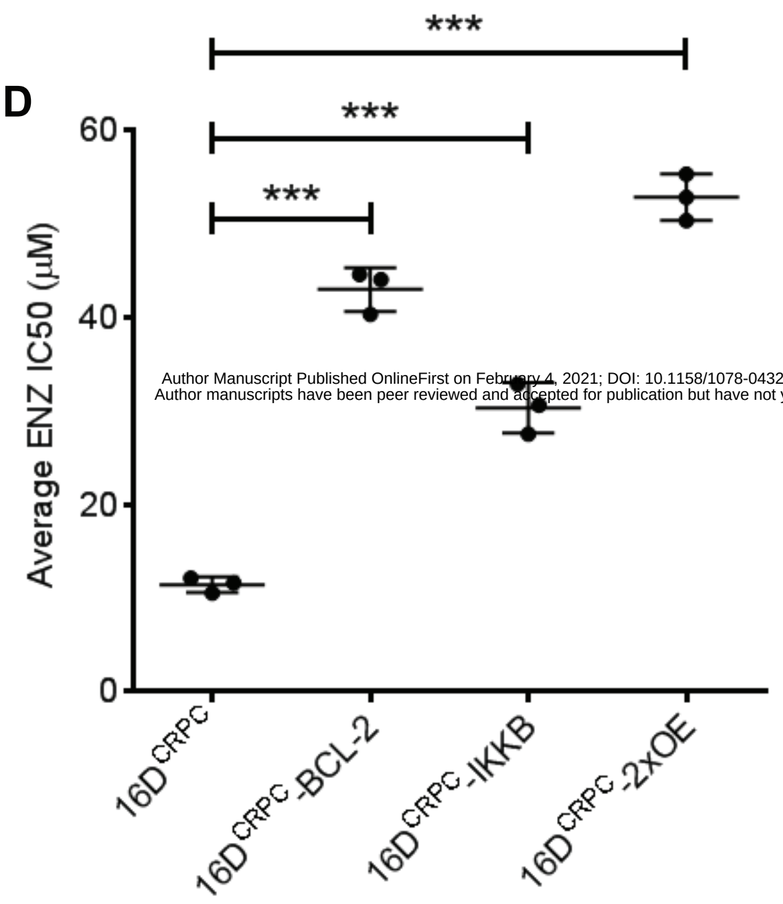

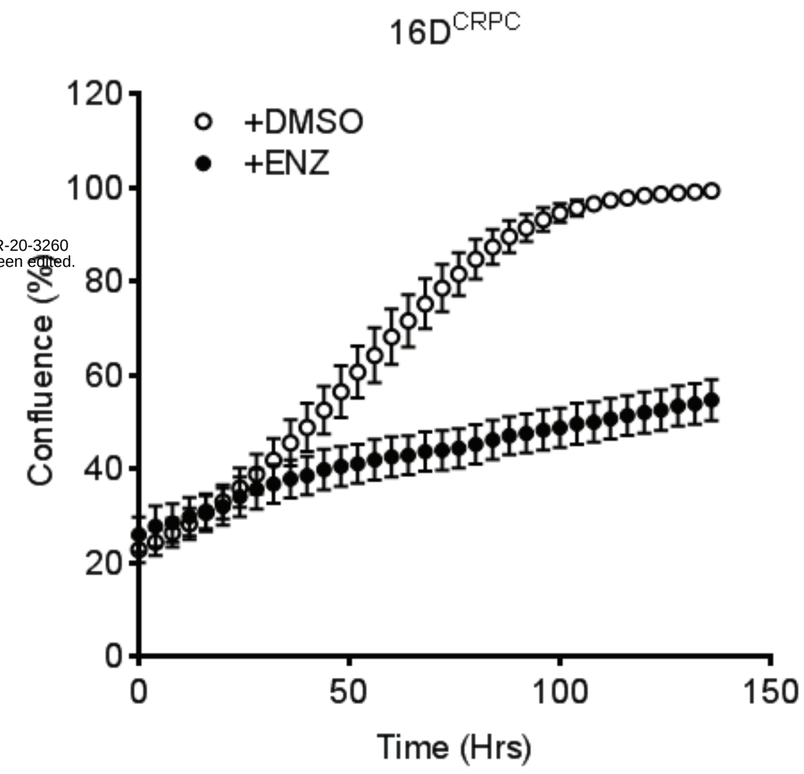

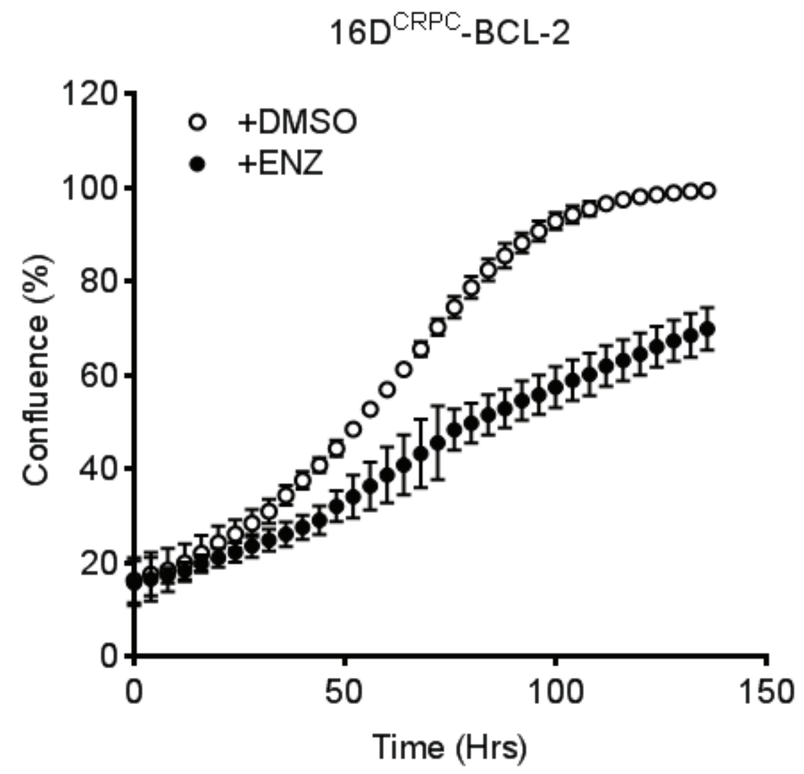

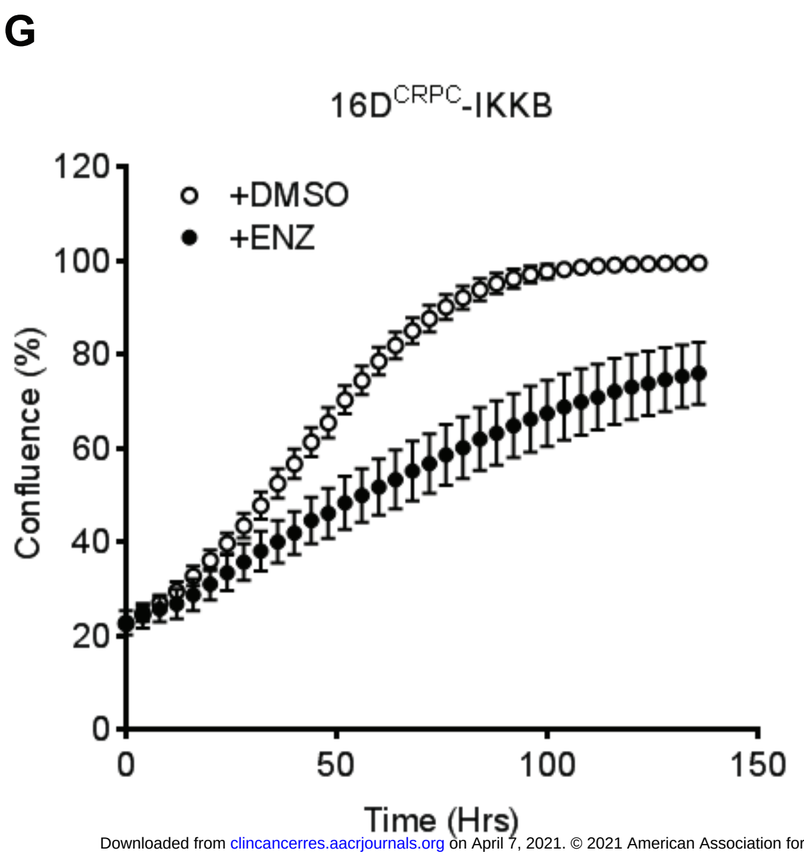

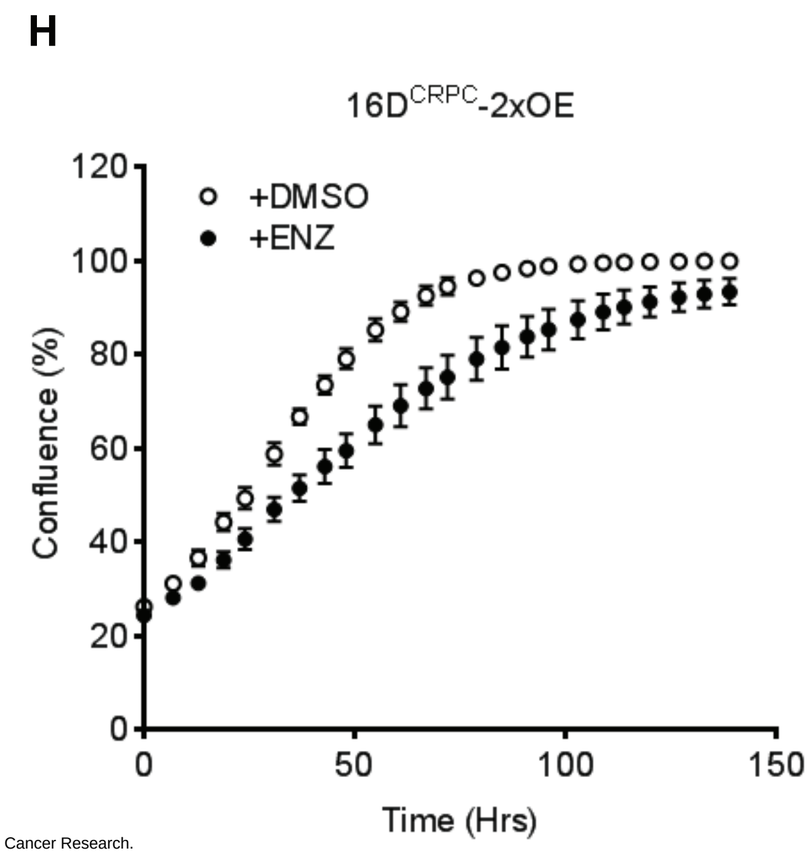

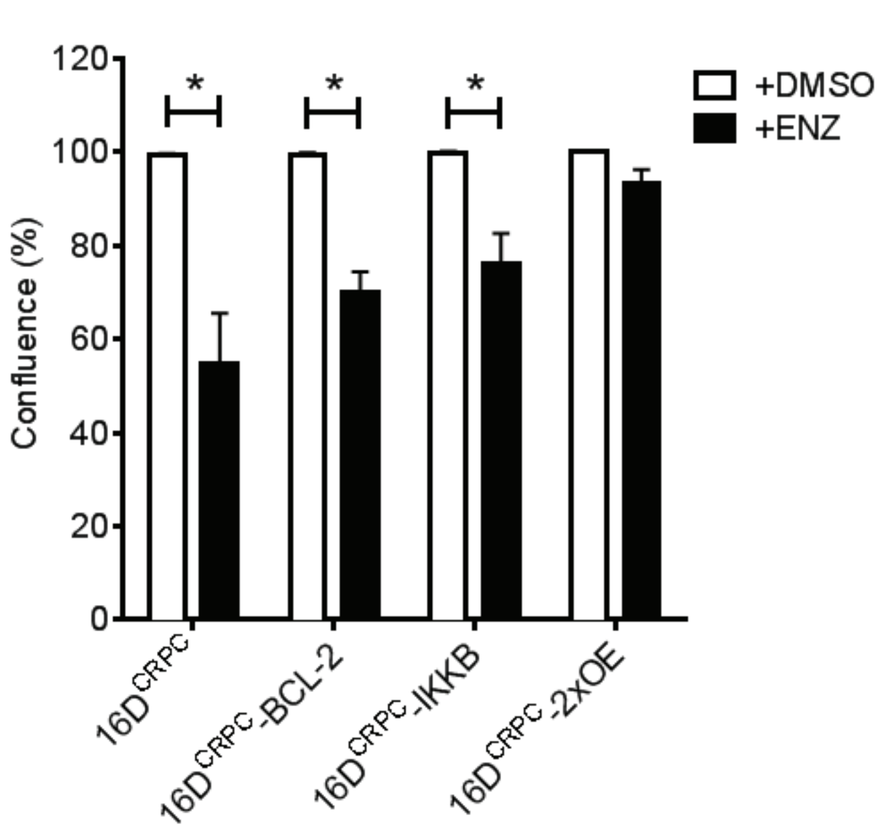

Fig. 4

A

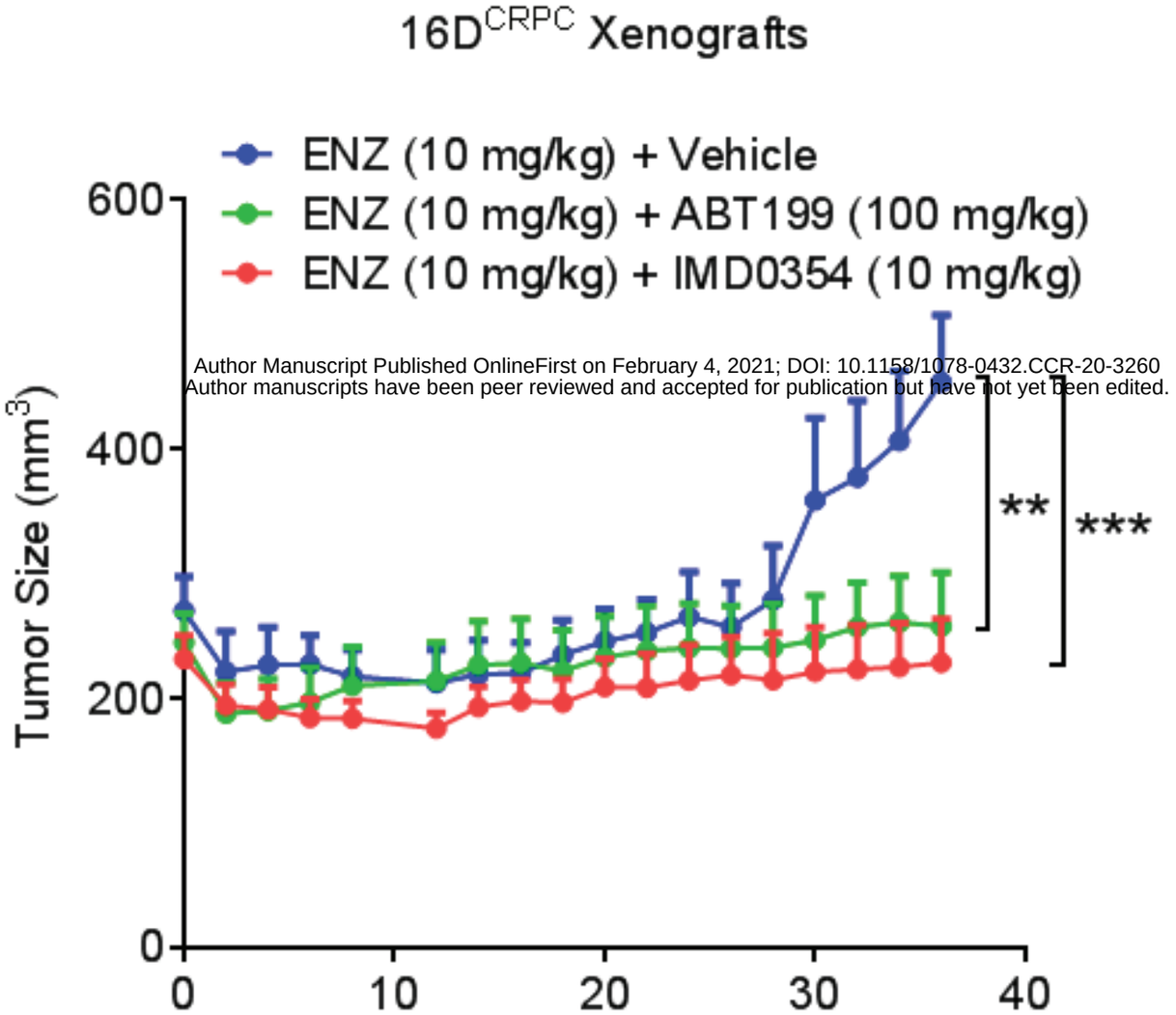

Author Manuscript Published OnlineFirst on February 4, 2021; DOI: 10.1158/1078-0432.CCR-20-3260
Author manuscripts have been peer reviewed and accepted for publication but have not yet been edited.

B

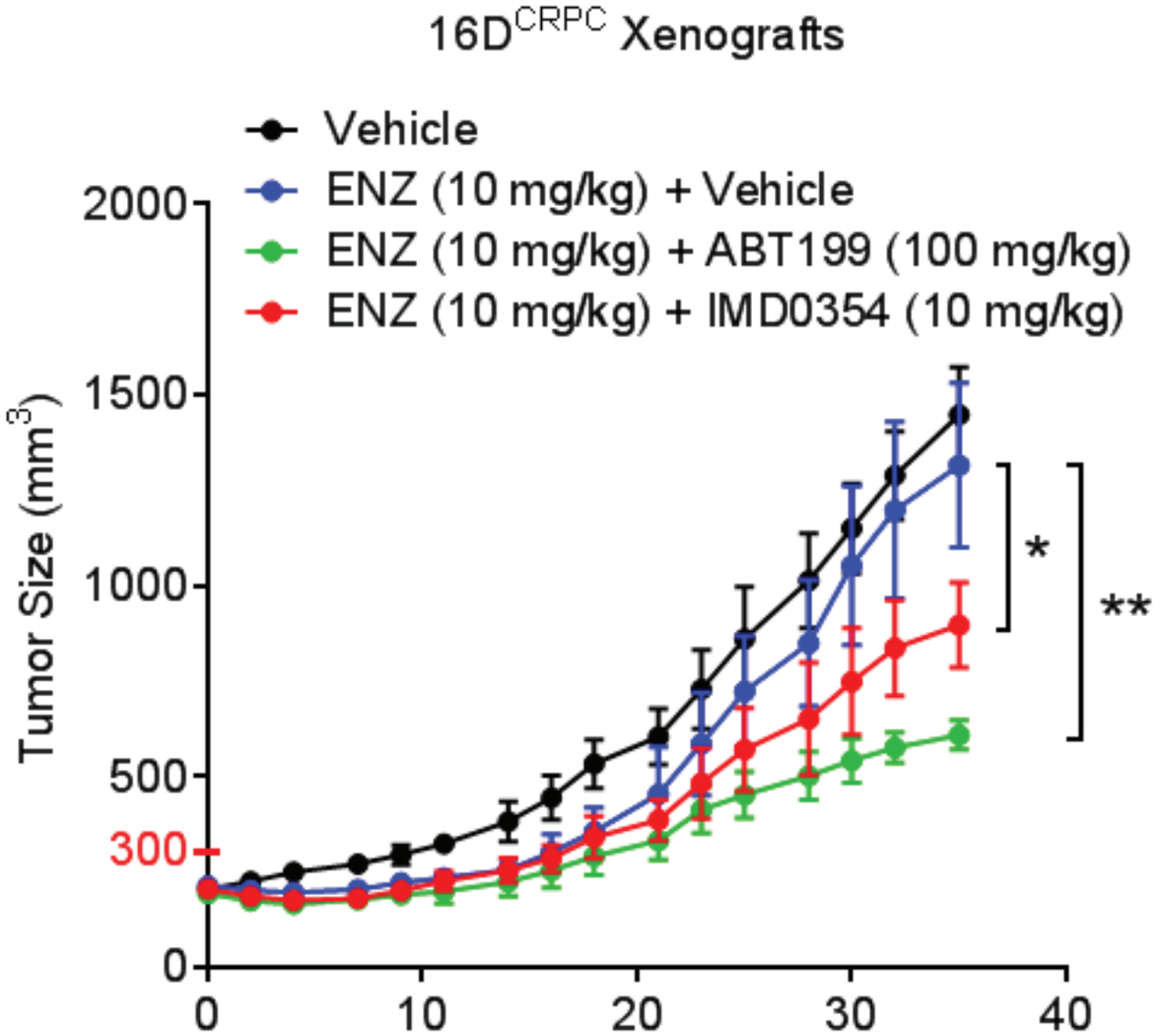

C

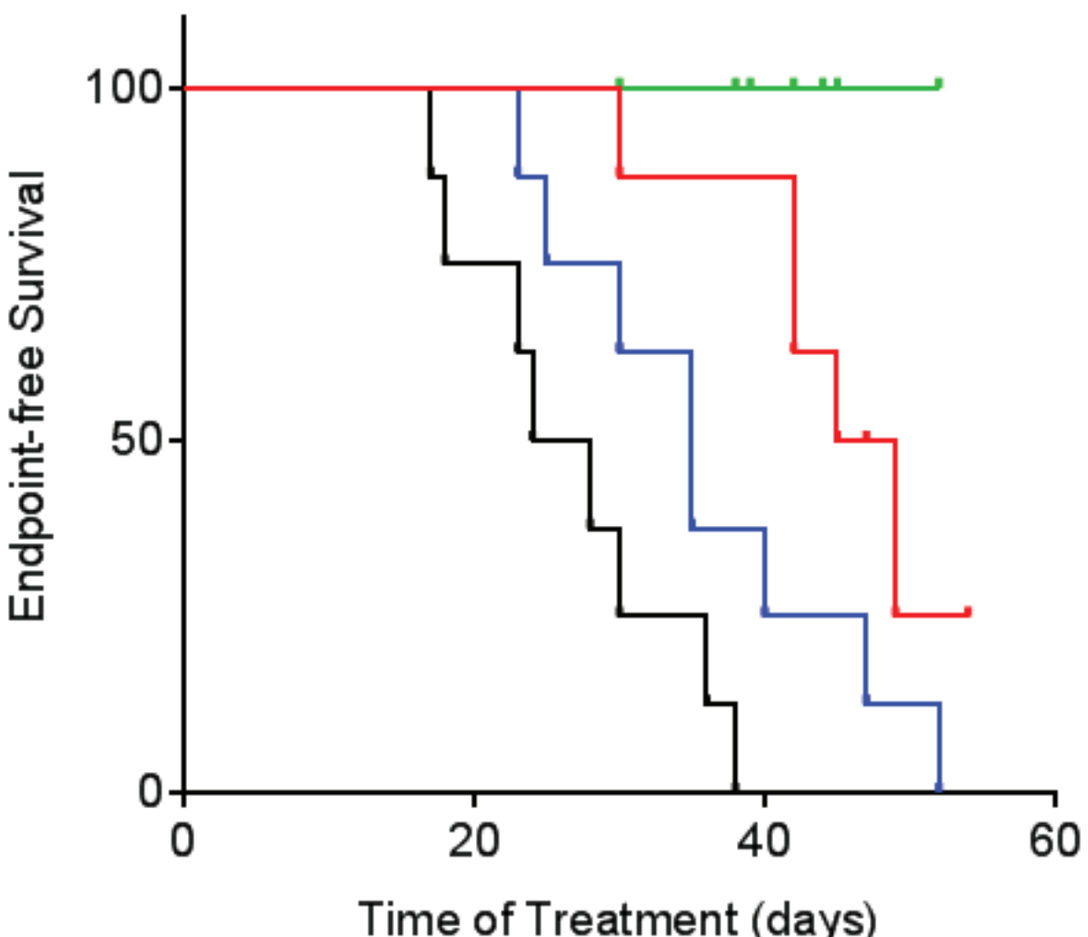

D

Pair-wise	Vehicle vs.			ENZ + Vehicle vs.	
	ENZ + Vehicle	ENZ + ABT199	ENZ + IMD0354	ENZ + ABT199	ENZ + IMD0354
p-value	**0.064**	**0.0001**	**0.0002**	**0.017**	**0.067**

Fig. 5

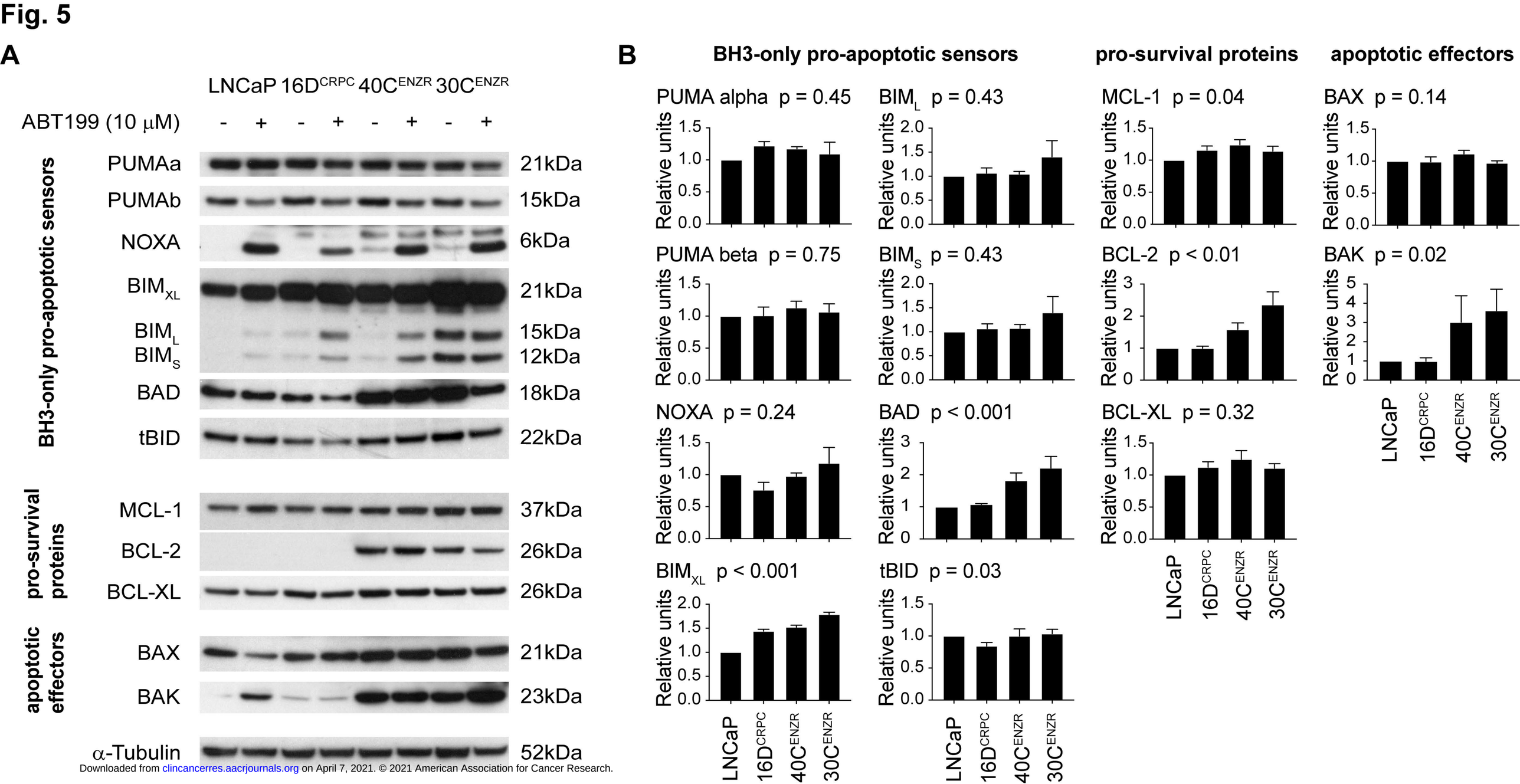

Fig. 6

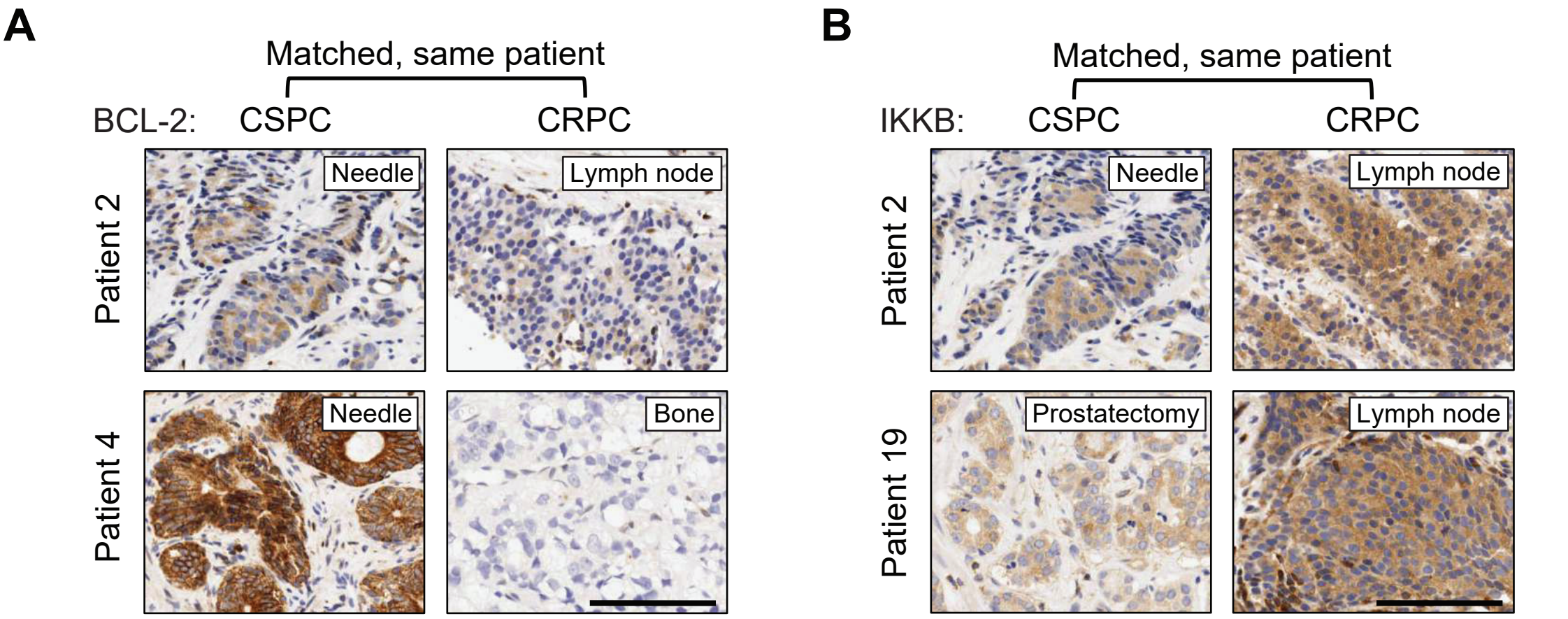

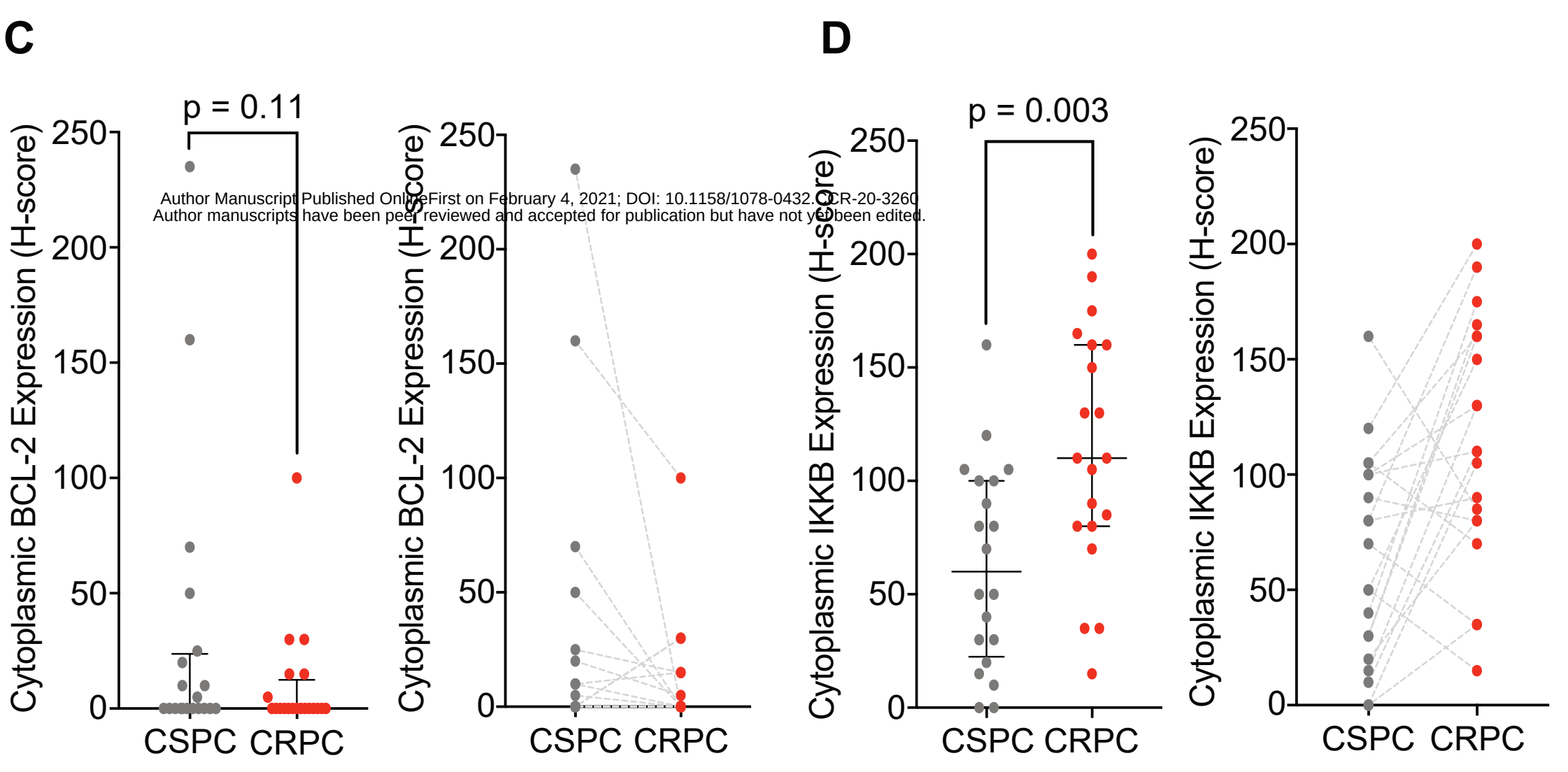

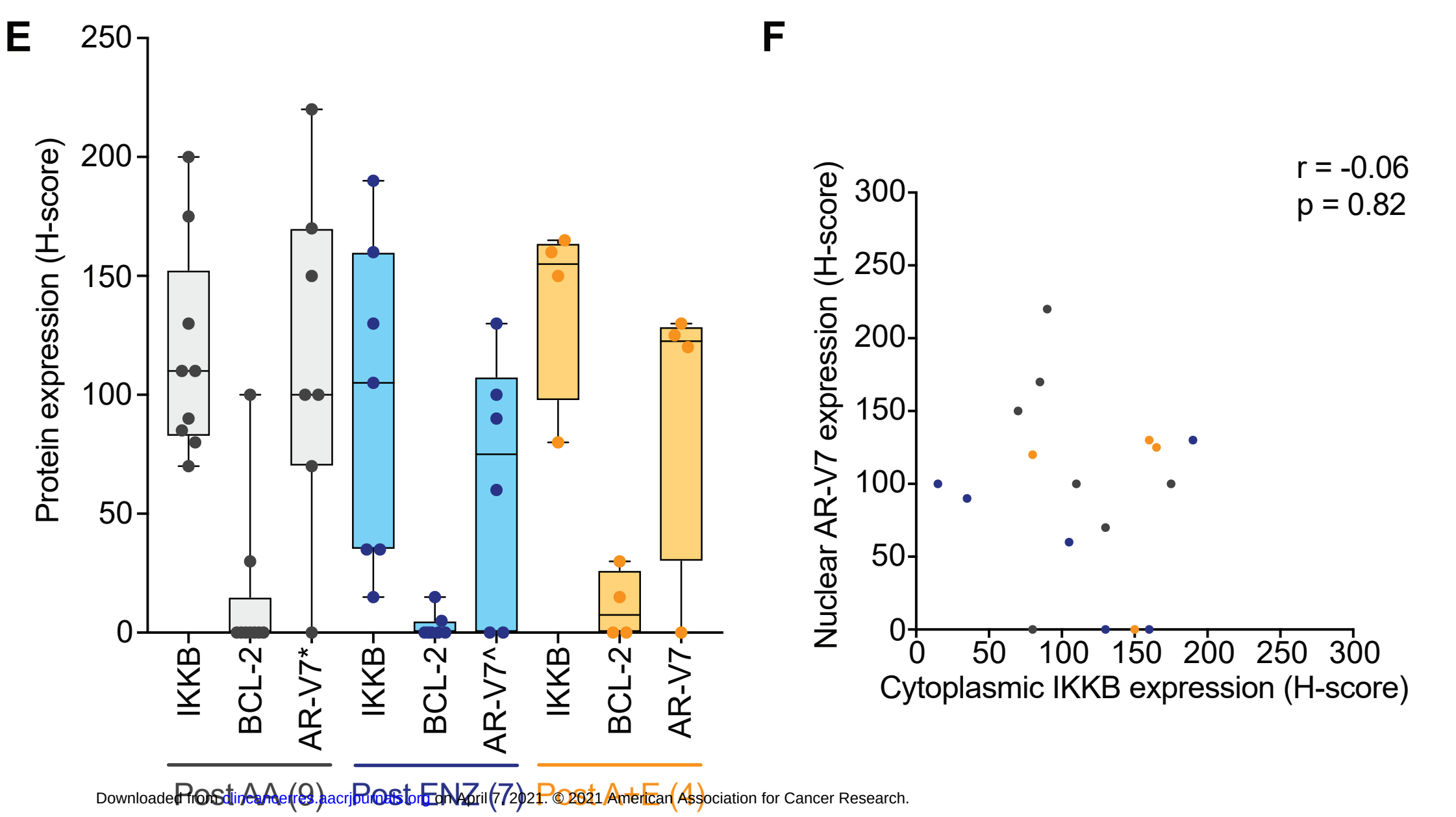

AACR American Association for Cancer Research

Clinical Cancer Research

Emergence of Enzalutamide resistance in prostate cancer is associated with BCL-2 and IKKB dependencies

Yi Liang, Sujeeve Jeganathan, Stefano Marastoni, et al.

Clin Cancer Res Published OnlineFirst February 4, 2021.